Biogeosciences, 21, 5495–5515, 2024
https://doi.org/10.5194/bg-21-5495-2024


Biogeosciences Open Access EGU



# Responses of field-grown maize to different soil types, water regimes, and contrasting vapor pressure deficit

**Thuy Huu Nguyen[1], Thomas Gaiser[1], Jan Vanderborght[3], Andrea Schnepf[3], Felix Bauer[3], Anja Klotzsche[3], Lena Lärm[3], Hubert Hüging[1], and Frank Ewert[1,2]**

[1]Institute of Crop Science and Resource Conservation (INRES), University of Bonn, Katzenburgweg 5, 53115 Bonn, Germany
[2]Leibniz Centre for Agricultural Landscape Research (ZALF), Institute of Landscape Systems Analysis, Eberswalder Straße 84, 15374 Müncheberg, Germany
[3]Agrosphere (IBG-3), Institute of Bio- and Geosciences, Forschungszentrum Jülich GmbH, 52428, Jülich, Germany

**Correspondence:** Thuy Huu Nguyen (tngu@uni-bonn.de)

Received: 8 December 2023 – Discussion started: 4 January 2024
Revised: 21 September 2024 – Accepted: 21 October 2024 – Published: 11 December 2024

**Abstract.** Drought is a serious constraint on crop growth and production of important staple crops such as maize. Improved understanding of the responses of crops to drought can be incorporated into cropping system models to support crop breeding, varietal selection, and management decisions for minimizing negative impacts. We investigate the impacts of different soil types (stony and silty) and water regimes (irrigated and rainfed) on hydraulic linkages between soil and plant, as well as root : shoot growth characteristics. Our analysis is based on a comprehensive dataset measured along the soil–plant–atmosphere pathway at field scale in two growing seasons (2017 and 2018) with contrasting climatic conditions (low and high vapor pressure deficit). Roots were observed mostly in the topsoil (10–20 cm) of the stony soil, while more roots were found in the subsoil (60–80 cm) of the silty soil. The difference in root length was pronounced at silking and harvest between the soil types. Total root length was 2.5–6 times higher in the silty soil than in the stony soil with the same water treatment. At silking time, the ratios of root length to shoot biomass in the rainfed plot of the silty soil (F2P2) were 3 times higher than those in the irrigated silty soil (F2P3), while the ratio was similar for two water treatments in the stony soil. With the same water treatment, the ratios of root length to shoot biomass of silty soil were higher than for stony soil. The seasonally observed minimum leaf water potential ($\psi_{leaf}$) varied from around $-1.5$ MPa in the rainfed plot in 2017 to around $-2.5$ MPa in the same plot of the stony soil in 2018. In the rainfed plot, the minimum $\psi_{leaf}$ in the stony soil was lower than in the silty soil from $-2$ to $-1.5$ MPa in 2017, respectively, while these were from $-2.5$ to $-2$ MPa in 2018, respectively. Leaf water potential, water potential gradients from soil to plant roots, plant hydraulic conductance ($K_{soil\_plant}$), stomatal conductance, transpiration, and photosynthesis were considerably modulated by the soil water content and the conductivity of the rhizosphere. When the stony soil and silt soil are compared, the higher "stress" due to the lower water availability in the stony soil resulted in fewer roots with a higher root tissue conductance in the soil with more stress. When comparing the rainfed with the irrigated plot in the silty soil, the higher stress in the rainfed soil resulted in more roots with a lower root tissue conductance in the treatment with more stress. This illustrates that the "response" to stress can be completely opposite depending on conditions or treatments that lead to the differences in stress that are compared. To respond to water deficit, maize had higher water uptake rate per unit root length and higher root segment conductance in the stony soil than in the silty soil, while the crop reduced transpired water via reduced aboveground plant size. Future improvements in soil–crop models in simulating gas exchange and crop growth should further emphasize the role of soil textures on stomatal function, dynamic root growth, and plant hydraulic system together with aboveground leaf area adjustments.

**Published by Copernicus Publications on behalf of the European Geosciences Union.**

## 1 Introduction

Maize (*Zea mays* L.) is a major staple crop throughout the world. Drought stress, which negatively affects crop growth and yield, is of increasing concern in several important maize-cultivating regions (Daryanto et al., 2016). Increases in frequency and severity of drought events due to climate change have been recently reported (IPCC, 2022). Thus, field observations and understanding on how maize responds to water stress are necessary to suggest promising traits for breeding programs (Vadez et al., 2021) as well as irrigation schemes (Fang and Su, 2019; Q. Cai et al., 2017). Improved understanding of crops' response to drought can be incorporated into soil–crop models (e.g., crop modeling and soil–vegetation–atmosphere transfer modeling).

Stomatal regulation is often considered a key aboveground hydraulic variable in regulating water use of crops. Maize is known as an isohydric plant. Maize stomata are closed in response to drought conditions to maintain leaf water potential ($\psi_{leaf}$) above critical levels ($\psi_{threshold}$ or minimum $\psi_{leaf}$) (Tardieu and Simonneau, 1998). The isohydric behavior is due to different mechanisms including hydraulic and/or chemical (e.g., abscisic acid (ABA)) signals (Tardieu, 2016). The degree to which these underlying mechanisms interact and differ among genotypes and/or environmental scenarios in explaining the stomatal regulation is still debated (Tardieu, 2016; Hochberg et al., 2018). Field evidence of variation in the minimum $\psi_{leaf}$ of maize due to soil water availability and soil hydraulics is rarely reported.

Water flow along the soil–plant–atmosphere continuum is determined by a series of hydraulic conductivities and gradients in water potential. Hydraulic conductance of soil ($K_{soil}$), root hydraulic conductance ($K_{root}$), and stem hydraulic conductance ($K_{stem}$) determine water potential from soil to root and root xylem water and thus magnitude of $\psi_{leaf}$. There are two main resistances to water flow from the soil to the shoot, namely the soil and the root resistances, often expressed as their inverse, $K_{soil}$ and $K_{root}$ (Nguyen et al., 2020; Cai et al., 2018). In wet soils, the soil hydraulic conductivity is much higher than that of roots, and water flow is mainly controlled by root hydraulic conductivity (Hopmans and Bristow, 2002; Draye et al., 2010). It is well known that a decrease in soil matric potential and soil hydraulic conductivity triggers stomatal closure and thus results in reduction in transpiration rate (Sinclair and Ludlow, 1986; Carminati and Javaux 2020; Abdalla et al., 2021). For the root water uptake and controlling stomata, the location where soil and roots are in close contact (rhizosphere) is most important, because when this thin layer of rhizosphere is disconnected (i.e., soil–root contact is lost), the water movement from soil toward the roots is reduced, which might trigger stomatal closure to maintain hydraulic integrity of the plant (Carminati et al., 2016; Rodriguez-Dominguez and Brodribb, 2020; Abdalla et al., 2022). The magnitude of the drop in water potential between bulk soil and soil–root interface increases considerably at different levels of soil dryness for different soil types (Carminati and Javaux, 2020; Abdalla et al., 2022). Hydraulic limits in the soil (Carminati and Javaux, 2020), in the root–soil interface (as measured for olive trees by Rodriguez-Dominguez and Brodribb, 2020, or tomato by Abdalla et al., 2022), in the root properties (Bourbia et al., 2021; Cai et al., 2022a; Nguyen et al., 2020; Cai et al., 2018), or due to both soil textures and root phenotypes (Cai et al., 2022b) emphasized the importance of belowground hydraulics (Carminati and Javaux, 2020). However, also the shoot hydraulic conductance could be limiting in some crop plants (Gallardo et al., 1996) or in trees (Domec and Pruyn, 2008; Tsuda and Tyree, 1997). Stomatal conductance and shoot hydraulic conductance showed close links to each other in pine trees (Hubbard et al., 2001). This summary illustrates three points:

i. Current studies have often focused either on above or on below hydraulic limits but rarely have considered both.

ii. The roles and relations of soil hydraulic properties to root and plant hydraulic conductance (and thus influences on stomatal conductance) remain unclear.

iii. The role of different hydraulic processes across the soil–plant–atmosphere continuum (i.e., soil to roots, stem, and soil–plant hydraulic conductance) in controlling stomatal conductance remains unclear.

Simultaneous measurements of atmospheric conditions (light intensity and vapor pressure deficit), leaf water potential, and transpiration rates, coupled with measurements of root, stem and whole-soil–plant hydraulic conductance, root architecture, and soil water potential distribution could reveal the relative importance of rhizosphere, shoot and root growth, and hydraulic conductance vulnerability, especially under progressive soil drying at field conditions (Carminati and Javaux, 2020; Tardieu et al., 2017). For the soil water conditions, soil texture and hydraulic characteristics are very important because they influence soil water movement and thus affect infiltration, surface and subsurface runoff, and ultimately plant available soil water (Vereecken et al., 2016). Soil texture properties, characterized by different fractions of clay, silt, and sand particles, are important drivers in determining the soil water retention properties (Scharwies and Dinneny, 2019; Stadler et al., 2015; Zhuang et al., 2001). Soil with higher water-holding capacity (here the silty soil with low stone content) has a larger amount of plant available water, which in turn enables crops to better meet the evaporative demand and facilitates better crop growth than the soil with high stone content (Nguyen et al., 2020; Cai et al., 2018). Estimations of hydraulic conductance (different organs and whole-plant hydraulic conductance) were done for crop plants and maize mainly under a controlled environment or pot conditions, e.g., for different species and genotypes during soil drying (Sunita et al., 2014; Choudhary and Sinclair, 2014; Abdalla et al., 2022; Meunier et al., 2018; Wang

et al., 2017; Li et al., 2016) or various species and genotypes together with different soil textures (Cai et al., 2022a), or soil texture with different vapor pressure deficit (VPD) (Cai et al., 2022b). Compared to the substantial effect of soil texture, there was no evidence of an effect of VPD on both soil–plant hydraulic conductance and on the relation between canopy stomatal conductance and soil–plant hydraulic conductance in pot-grown maize (Cai et al., 2022b). Contrast results were found in winter wheat where plant hydraulic conductance increased with rising VPD for some genotypes in wet conditions (Ranawana et al., 2021). Vadez et al. (2021) examined the effects of soil types together with increasing VPD on transpiration efficiency (TE) and yield under pot conditions for several $C_4$ species (maize, sorghum, and millet). The interpretation of differences in TE was attributed to soil types, more specifically to the differences in soil hydraulic properties and soil hydraulic conductance. However, experimental evidence linking root hydraulics to stomatal regulation was lacking in these two Vadez studies (Vadez et al., 2021). Recent field studies have aimed at quantification of root hydraulic conductance and its linkages with crop growth (leaf area and biomass) under different soil types (wheat in G. Cai et al., 2017; Cai et al., 2018; Nguyen et al., 2020, or maize in Nguyen et al., 2022a; Jorda et al., 2022). However, field studies that consider both below (soil–root hydraulic conductance) and above (stem hydraulic conductance) parts, or soil–plant hydraulic conductance (including below- and aboveground parts) and their roles in stomatal regulation as well as crop growth (leaf area and biomass) are rarely carried out.

This study aims at further understanding of the hydraulic linkages between soil and plant and responses of plants to drought stress in relation to root : shoot growth characteristics at field scale. We hypothesize that, in field-grown maize, (1) soil–plant hydraulic conductance depends on soil hydraulic properties, especially under dry soil conditions, and (2) minimum leaf water potential of maize is similar across soil types, water treatments, and climatic conditions. The hypotheses will be tested with three objectives: (i) to investigate the effects of soil types, water application, and climatic condition on root growth; (ii) to investigate the effects of soil types, water application, and climatic condition on stomatal conductance, leaf photosynthesis, transpiration, leaf water potential, different components of the hydraulic conductance (root, stem, and whole soil–plant); and (iii) to analyze the relative contribution of root and shoot growth (leaf area and biomass) on the water uptake capacity of maize. These three objectives will be achieved based on a comprehensive dataset covering the whole-soil–plant continuum over two growing maize seasons with contrasting climatic conditions (low and high VPD) under two water treatments (rainfed and irrigated) and two different soil types (stony and silty soil).

## 2 Materials and methods

### 2.1 Location and experimental setup

We carried out a field experiment at two rhizotron facilities in Selhausen, North Rhine-Westphalia, Germany (50°52′ N, 6°27′ E). The field is slightly inclined with a maximum slope of around 4°. One rhizotron facility was located upslope (F1) with around 60 % gravel by weight in the 10 cm topsoil, while the second rhizotron facility was downslope (F2) with silty soil (stone content is around 4 % by weight).

Each rhizotron facility was divided into three subplots of 7.25 m by 3.25 m: two rainfed plots (P1, P2), and one irrigated plot (P3). In rainfed plot P1, other sowing densities and dates were used than in the other plots, and we therefore excluded these plots. Silage maize *Zea mays* L. 'Zoey' was sown on 4 and 8 May in 2017 and 2018, respectively, with a plant density of 10.66 seeds $m^{-2}$ (Fig. 1a; Table 1). Detailed information on crop management practices is provided in Table 1.

### 2.2 Water application

The irrigation systems (T-Tape 520-20-500 drip lines (Wurzelwasser GbR, Müzenberg, Germany)) were installed parallel to the crop rows with 0.3 m intervals. A nearby weather station (approx. 100 m from the experiment) recorded weather variables (global radiation, temperature, relative humidity, precipitation, and wind speed) every 10 min. In addition, the precipitation amount was manually collected by a plastic rain gauge next to each rhizotron facility. The Penman–Monteith equation was employed to estimate reference evapotranspiration. Daily crop evapotranspiration was calculated based on the single crop coefficient and the reference evapotranspiration (Allen et al., 1998). Irrigation amounts were estimated as the weekly sum of the calculated crop evapotranspiration. A total amount of 230 mm precipitation was recorded during the growing period (136 d), while average, minimum, and maximum daily air temperatures were 17.6, 8.3, and 25.3 °C, respectively (Fig. 1b). The crop on the irrigated plots (2017F1P3 and 2017F2P3) received in total 130 mm (10 times, every 5–7 d, using 13 mm of irrigation water per event) between mid-June to the end of August (Fig. 1b). Average, minimum, and maximum daily air temperatures in 2018 were higher than in 2017 with 19.2, 10.85, and 27.3 °C, respectively (Fig. 1b). The summer season in 2018 could be considered an extreme year with respect to plant growth at our experimental location due to exceptionally hot and dry weather conditions. The crop received only 91.3 mm of rain during the growing period of 2018 (107 d). The crop on the irrigated plots 2018F1P3 and 2018F2P3 was irrigated every 5–7 d (in total 13 times), with a total amount of irrigation of 257 and 239 mm between mid-June and mid-August, respectively (Fig. 1d). To avoid crop failure due to severe drought in 2018, the rainfed plot

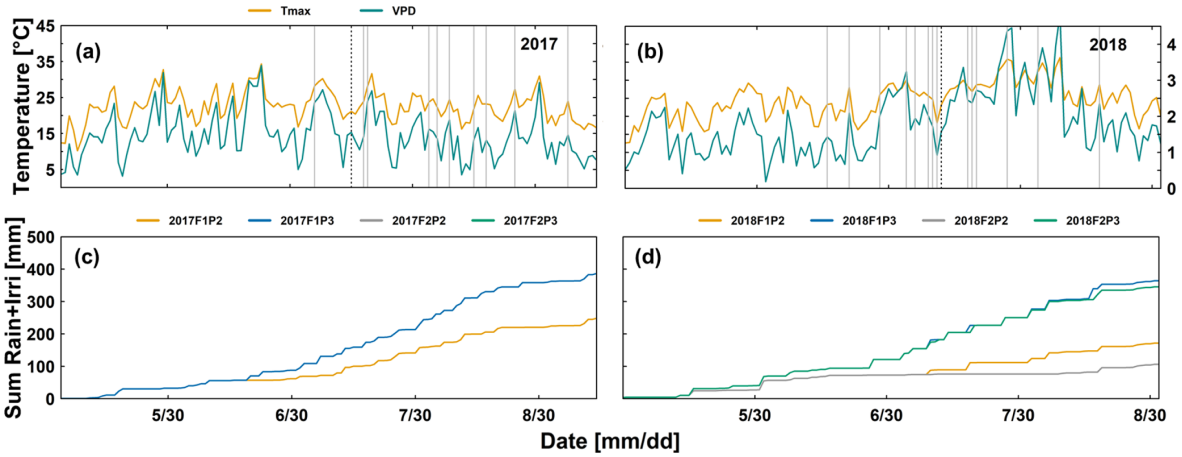


**Figure 1.** Daily maximum air temperature ($T_{max}$) (°C), daily maximum air vapor pressure deficit (VPD) (kPa) in the two growing seasons in **(a)** 2017 and **(b)** 2018, and cumulative (sum) of rainfall and irrigation from the rainfed (P2) and irrigated (P3) plots of the stony soil (F1) and silty soil (F2) in the two growing seasons in **(c)** 2017 and **(d)** 2018. The vertical dashed black lines in **(a)** and **(b)** indicate silking time. Vertical grey lines in **(a)** and **(b)** indicate the measured days for leaf gas exchange and leaf water potential. Two lines for 2017F2P2 and 2017F2P3 are overlapped by the lines from 2017F1P2 and 2017F1P3, respectively.

**Table 1.** Crop phenology and management information for different treatments in 2017 and 2018. Dates follow the format mm/dd.

| | 2017 | | | | 2018 | | | |
|---|---|---|---|---|---|---|---|---|
| Soil types | Stony (F1) | Stony (F1) | Silty (F2) | Silty (F2) | Stony (F1) | Stony (F1) | Silty (F2) | Silty (F2) |
| Water treatments | Rainfed (P2) | Irrigated (P3) | Rainfed (P2) | Irrigated (P3) | Rainfed (P2) | Irrigated (P3) | Rainfed (P2) | Irrigated (P3) |
| Plot names | F1P2 | F1P3 | F2P2 | F2P3 | F1P2 | F1P3 | F2P2 | F2P3 |
| Growing season (days)[a] | 136 | 136 | 136 | 136 | 107 | 107 | 107 | 107 |
| Cumulative rainfall (mm)[b] | 248.7 | 248.7 | 248.7 | 248.7 | 91.3 | 91.3 | 91.3 | 91.3 |
| Irrigation (mm) | 0 | 130 | 0 | 130 | 66 | 257.6 | 0 | 257.6 |
| Fertilizer application (per hectare) | 05/09: 100 kg N + 40 kg $P_2O_5$<br>07/06: 80 kg N + 40 kg $K_2O$ | | | | 05/22: 100 kg N<br>05/30: 40 kg $P_2O_5$ + 40 kg $K_2O$<br>06/27: 80 kg N | | | |
| Sowing date | 05/04 | | | | 05/08 | | | |
| Emergence date | 05/09 | | | | 05/13 | | | |
| Tasseling date | 07/09 | | | | 07/09 | | | |
| Silking date | 07/14 | | | | 07/11 | | | |
| Harvest date | 09/12 | | | | 08/22 | | | |

[a] From sowing to harvest. [b] For rainfall for the whole growing season.

in the stony soil (2018F1P2) had to be irrigated (in total 66 mm) four times (using 13, 22, 13, and 18 mm, respectively) (Fig. 1d). Detailed estimates of irrigation amount and intervals could be found in Nguyen et al. (2022a).

### 2.3 Measurements

#### 2.3.1 Soil water measurement and root growth

MPS-2 matrix water potential and temperature sensors (Decagon Devices Inc.; UMS GmbH, Munich, Germany) were installed at soil depths of 10, 20, 40, 60, 80, and 120 cm to measure half-hourly soil water potential and soil temperature. The range of the water potential measurements is from −9 kPa to approximately −100 000 kPa (1.96 to 6.01 pF). In addition to MPS-2, soil water potential was measured by pressure transducer tensiometers (T4e, UMS GmbH, Munich, Germany) where the minimum detectable suction is −85 to +100 kPa. A detailed description of sensor installation, calibration, and data post-processing can be found in Cai et al. (2016).

Minirhizotubes (7 m long clear acrylic glass tubes with outer and inner diameters of 6.4 and 5.6 cm, respectively) were installed horizontally at six different depths of 10, 20, 40, 60, 80, and 120 cm below the soil surface in each facility. There are three replicate tubes at each depth, accounting for 54 tubes in each facility. Root measurements were taken manually by a Bartz camera (Bartz Technology Corporation) (23 June–12 September 2017) and a VSI camera (Vienna Scientific Instruments GmbH) (8–22 June 2017) in 2017, while only a VSI was used in 2018 (23 May–23 August 2018). Root images were taken at 20 fixed positions from the left- and right-hand sides of each tube weekly (or biweekly) during the growing seasons. The root images were analyzed by an automated minirhizotube image analysis pipeline for segmentation and automated feature extraction (Bauer et al., 2021). Two-dimensional root length density (RLD, in units of $\mathrm{cm\,cm^{-2}}$) was estimated from the total root length observed in the image and the image surface area. The overview of camera system, minirhizotube images acquisition, and post-processing of the root data are described in detail in Bauer et al. (2021) and Lärm et al. (2023).

#### 2.3.2 Crop growth, leaf gas exchange, leaf water potential, and sap flow measurements

The phenology, plant height, stem diameter, green and brown leaf area, dry matter of different organs, and total aboveground dry matter were observed and measured biweekly. Dates of sowing, emergence, tasseling, and silking for two growing seasons were observed. There was a difference in emergence, tasseling, and silking dates for two growing seasons due to the differences in sowing dates and temperature. However, the developmental stages were not different among water treatments and soil types within one season. Measurements of green leaf area and aboveground dry matter were based on the destructive method.

We performed leaf gas measurements under clear-sky and sunny conditions. Hourly leaf stomatal conductance (Gs), net photosynthesis (An), and leaf transpiration ($E$) of two sunlit leaves (uppermost fully developed leaves) and one shaded leaf of different plants were measured every 2 weeks. The Gs, An, and $E$ were measured at steady state using a LI-COR 6400 XT device (LI-COR Biosciences, Lincoln, Nebraska, USA). Leaf water potential ($\psi_{\mathrm{leaf}}$) was measured with a pressure chamber (SKPM 140/(40-50-80), Skye Instrument Ltd, UK).

Based on stem diameter size, 20 sap flow sensors (SGA 13, SGB 16, and SGB 19 types) were installed (one sensor per plant and five maize plants per treatment) each year. The sensors were operated from 7 July 2017 and from 28 June 2018 until harvest for the 2017 and 2018 growing season, respectively. The calculated sap flow in the plant ($\mathrm{g\,h^{-1}}$) from the data loggers (Dynamax, 2005) was used to compute canopy transpiration based on the plant density per square meter. Further details on developmental stages, crop growth, leaf gas exchange, leaf water potential, and sap flow measurements can be found in Nguyen et al. (2024, 2022a, 2020).

### 2.4 Calculation of total root length, root system conductance, stem, and whole-plant hydraulic conductance

To estimate the total root length from minirhizotubes, we adopted option 2, which was described in G. Cai et al. (2017). Total root length per square meter soil surface area within each soil layer ($\mathrm{m\,m^{-2}}$) was computed by multiplying the root length density with the corresponding soil layer thickness. The root length density was determined in each depth by dividing the measured root length per minirhizotron image by the assumed volume the roots would have occupied in absence of the tube, i.e., $W \cdot L \cdot$ tube radius (see G. Cai et al., 2017).

Following Nguyen et al. (2020), the effective soil water potential was calculated based on hourly measured soil water potential ($\psi_i$) and normalized root length density at six depths (10, 20, 40, 60, 80, and 120 cm) ($\mathrm{NRLD}_i$) and soil layer thickness ($\Delta z_i$) in the soil profile (Eq. 1).

$$\psi_{\mathrm{soil\_effec}} = \sum_{i=1}^{N} \psi_i \mathrm{NRLD}_i \Delta z_i \quad (1)$$

We followed Ohm's law analogy by dividing the hourly sap flow by the difference between effective soil water potential and shaded leaf water potential to estimate root system conductance ($K_{\mathrm{soil\_root}}$ – Eq. 2), between shaded leaf water potential and sunlit leaf water potential to estimate stem hydraulic conductance ($K_{\mathrm{stem}}$ – Eq. 3), and between effective soil water potential and sunlit leaf water potential to estimate

whole-plant hydraulic conductance ($K_{soil\_plant}$ – Eq. 4).

$$K_{soil\_root} = \text{Sapflow} / \left(\psi_{soil\_effec} - \psi_{shadedleaf}\right) \quad (2)$$

$$K_{stem} = \text{Sapflow} / \left(\psi_{shadedleaf} - \psi_{sunlitleaf}\right) \quad (3)$$

$$K_{soil\_plant} = \text{Sapflow} / \left(\psi_{soil\_effec} - \psi_{sunlitleaf}\right) \quad (4)$$

During 1 measurement day, four values of the $K_{soil\_root}$, $K_{stem}$, and $K_{soil\_plant}$ were obtained from measurements between 11:00 and 14:00 CEST. The average and standard deviation of these hourly measurements were calculated for each measurement day in order to present the seasonal dynamics of those variables. To capture the diurnal and seasonal variations of sap flow and sunlit leaf water potential, in addition, we plotted the hourly sap flow and hourly difference in effective soil water potential and sunlit leaf water potential for 3 measurement days starting from predawn and whole seasons, respectively, to derive the slope, which is also $K_{soil\_plant}$.

### 2.5 Statistical analysis

Regression analysis was performed to understand the relationship between the sap flow volume and the difference in effective soil water potential and sunlit leaf water potential as well as the relationship between the total aboveground biomass and cumulated water transpired (sap flow volume). These analyses allow one to derive the slope as a proxy of $K_{soil\_plant}$ and transpiration use efficiency, respectively. Since all measured data have their own measurement errors, the generalized Deming regression was employed. We performed relationships (via correlation coefficient and statistical significant levels) of midday leaf An, Gs, and $E$ with midday $K_{stem}$, $K_{soil\_plant}$, $K_{soil\_root}$, sunlit leaf potential, $\psi_{soil\_effec}$, and the difference in $\psi_{soil\_effec}$ and sunlit leaf water potential ($\psi_{difference}$). All data processing and analyses were conducted using the R statistical software (R Core Team, 2022).

## 3 Results

### 3.1 Root growth under different water treatments, soil types, and climatic conditions

Observed root lengths (cm cm$^{-2}$) from the minirhizotubes at different soil depths in the first week of June (stem elongation), around silking, and at harvest in two growing seasons are shown in Fig. 2. Root length was similar among water treatments at the start of stem elongation in both years (Fig. 2a and d). The difference in root length was pronounced at silking and harvest between the soil types. More root growth was observed in the silty soil than in the stony soil with the same water treatment (i.e., 2.5–6 times higher at a depth of 40 cm). This indicated the strong negative effects of stone content on root development. In the stony soil, root length in the irrigated plot (F1P3) was slightly higher than

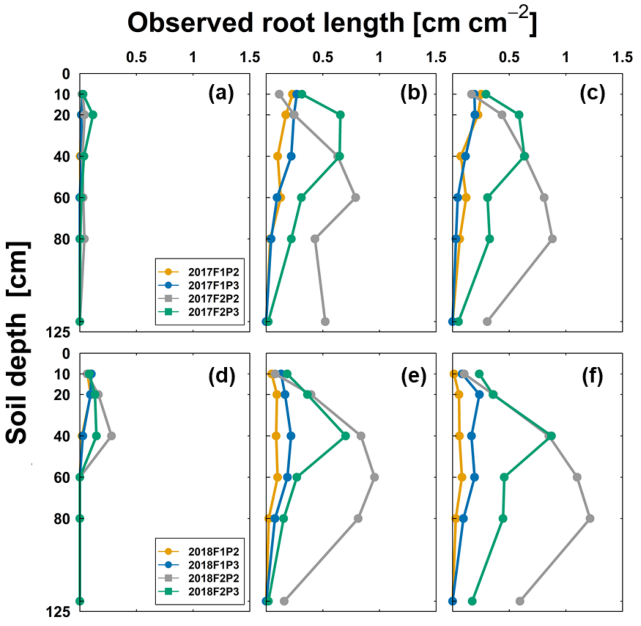


**Figure 2.** Observed root length from minirhizotubes (cm cm$^{-2}$) from 10, 20, 40, 60, 80, and 120 cm soil depth from the rainfed (P2) and irrigated (P3) plots of the stony soil (F1) and silty soil (F2) in the two growing seasons in 2017 (**a** – 8 June, **b** – at silking on 13 July, **c** – at harvest on 12 September) and in 2018 (**d** – 7 June, **e** – 1 week after silking – 18 July, **f** – 1 week before harvest – 16 August).

in the rainfed plot (F1P2). In contrast, the rainfed treatment (F2P2) in the silty soil showed much higher root length, especially from 40 to 120 cm depth, than the irrigated plot (F2P3) in both growing seasons. Much lower stone content and deep soil cracks in the silty soil (Morandage et al., 2021) allow root extension to the subsoil, particularly in the rainfed plot F2P2. Root length in the rainfed treatment (F2P2) in 2018 was higher than in 2017, which implies that root further developed to exploit the water in the soil under rainfed conditions to meet the higher evaporative demand.

Total root length (m m$^{-2}$) estimated from minirhizotubes and its ratio to shoot dry matter (m kg$^{-1}$) on three measured dates (as in Fig. 2) are shown in Fig. 3. Total root length was much higher for the silty plots than for stony plots. In 2017, the highest total root length was observed in the rainfed plot of the silty soil (F2P2) with approximately 9166 and 9878 m m$^{-2}$ around silking and harvest, respectively, which was almost 2 times higher than in the irrigated plot (F2P3). These figures were higher in 2018 than in 2017, where total root length of F2P2 was 10 188 m m$^{-2}$ and 13 750 m m$^{-2}$ at silking and harvest time, respectively. For the rainfed stony soil (F1P2), soil water depletion around the beginning of June 2017 (Fig. S1a in the Supplement) and from the first 2 weeks of June to harvest in 2018 (Fig. S2a) caused the strong reduction of shoot biomass. In the stony soil, the shoot dry matter of the irrigated plot (F1P3) and the rainfed plot (F1P2)

was 1275 and 536 g m$^{-2}$ at silking time (e.g., 19 July 2018 – DOY 200; Fig. S3a and b). However, there was a minor difference between F1P2 and F1P3 in terms of the ratio of root length to shoot dry matter. In the silty soil, a decrease in soil water potential was not pronounced (compared to stony soil) in either 2017 or 2018 (Figs. S1b and S2b). In 2018, shoot biomass in the irrigated stony soil (F1P3) and silt soil (F2P3) was similar (1275 and 1299 g m$^{-2}$, respectively on 19 July 2018 – DOY 200), while the shoot biomass of the rainfed silty soil (F2P2) was 876 g m$^{-2}$ (Fig. S3a and b). However, the ratios of root length to shoot biomass in the rainfed plot of the silty soil (F2P2) were 3 and 6 times higher than those in the irrigated silty soil (F2P3) and stony soil (F1P3), respectively (e.g., 18 July, DOY 199). Moreover, total root length was relatively equal among treatments at the start of set elongation (8 June – DOY 159) in both years, while this was the opposite for the ratio of root length to shoot dry matter. This firstly illustrated that the finer soil texture without stones and with soil cracks could favor the root growth, which indicates strong interactions of root and soil conditions. Secondly, the larger root length and higher atmospheric evaporative demand in 2018 than in 2017 also indicate the interaction of root growth and climatic conditions.

### 3.2 Stomatal conductance, photosynthesis, transpiration, and $K_{\text{soil\_plant}}$

#### 3.2.1 Diurnal course of stomatal conductance, photosynthesis, transpiration, and water potential at leaf level

After a long period with high temperatures and no rainfall, soil water reduction in the rainfed plot of the stony soil (F1P2) on 17 July 2018 (Fig. S2) resulted in 3 times lower net photosynthesis (An), stomatal conductance (Gs), transpiration ($E$), and leaf water potential ($\psi_{\text{leaf}}$) compared to the remaining treatments (Fig. S4). This indicates that the soil water content strongly affected the stomatal conductance. Stomatal closure was very pronounced around midday in F1P2, while this was not the case in F2P2, indicating the soil type strongly affected the stomatal conductance and leaf gas exchange. Leaf gas exchange and leaf water potential in F1P2 were still much lower than in other plots (Fig. 4). On 18 July 2018, after application of 22.75 mm of irrigation water (at 16:00), photosynthesis, stomatal conductance, transpiration, and leaf water potential were slightly increased in F1P2. However, these were still smaller than in F2P2 and the two irrigated plots.

On the next day after irrigation, leaf gas exchange and water potential were considerably increased in F1P2 (Fig. S5). Leaf curling was also less pronounced than the 2 previous days. Predawn and midday leaf water potentials were around $-0.4$ and $-1.6$ MPa for all plots, respectively. Leaf transpiration rate was around 3.1 mmol m$^{-2}$ s$^{-1}$ for all water treatments and soil types at 00:00. This indicated the recovery of the plant after watering at the rainfed plot with stony soil (F1P2).

#### 3.2.2 Seasonal course of stomatal conductance, photosynthesis, transpiration, water potential, and plant hydraulic conductance at the leaf level

Seasonal stomatal conductance (Gs) and leaf water potential ($\psi_{\text{leaf}}$) are described in Fig. 5. The relationship between two variables was rather noisy and nonlinear. The leaf water potential showed distinct patterns among treatments in one growing season. Minimum $\psi_{\text{leaf}}$ was maintained at around $-1.5$ MPa in the irrigated plot in the stony soil (F1P3) and two plots in the silty soil (F2P2 and F2P3). Lower minimum $\psi_{\text{leaf}}$ could be observed in the rainfed plot with stony soil (F1P2), but it did not go beyond $-2$ MPa. Minor leaf curling was observed only in the second week of June in F1P2 in 2017. In 2018, the higher temperature and vapor pressure deficit resulted in lower minimum $\psi_{\text{leaf}}$ in all treatments and soil types compared to 2017. The minimum $\psi_{\text{leaf}}$ was around $-2$ MPa in F1P3, F2P2, and F2P3, while $\psi_{\text{leaf}}$ could drop below $-2$ MPa in F1P2, which was due to the severe soil water deficit. The low Gs and $\psi_{\text{leaf}}$ were associated with measurement dates when the substantial leaf curling was observed from mid-July to the end of growing season in F1P2 in 2018 (Figs. S3c, d and S6c, d).

The effective soil water potential ($\psi_{\text{soil\_effect MD}}$), sunlit leaf water potential ($\psi_{\text{sunlitleaf MD}}$), stomatal conductance ($\text{Gs}_{\text{MD}}$), and whole-plant hydraulic conductance ($K_{\text{soil\_plant MD}}$) at midday at several times during the growing season are presented in Figs. 6 and 7 for 2017 and 2018, respectively. As expected, there was not much difference in terms of $\psi_{\text{soil\_effec MD}}$ among F1P3, F2P2, and F2P3 from 2 August to 1 week before harvest in 2017. The lowest $\psi_{\text{soil\_effec MD}}$ was observed in F1P2. Leaf water potential dropped drastically, but $K_{\text{soil\_plant MD}}$ also increased strongly, whereas $\psi_{\text{soil\_effec MD}}$ remained quite similar (e.g., 18 July). This is because sap flow increased substantially on this day (e.g., from 2.34 mm d$^{-1}$ on 17 July to 6.97 mm d$^{-1}$ on 18 July for the F1P2). The stomatal conductance decreased a lot on this day, which could be explained by the fact that the atmospheric demand increased (e.g., global radiation was 13.6 MJ m$^{-2}$ on 17 July compared to 23.9 MJ on 18 July while daily VPD was 0.7 and 1.2 kPa, respectively) even more than the sap flow. Midday sunlit leaf water potential was not distinctively different among treatments with the lowest $\psi_{\text{sunlitleaf MD}}$ around $-1.6$ MPa throughout season. Also, $\text{Gs}_{\text{MD}}$ was rather similar among plots. The $K_{\text{soil\_plant MD}}$ ranged from 0.125 to 0.96 mm h$^{-1}$ MPa$^{-1}$ with a sharp reduction before harvest. In general, the lowest values of $K_{\text{soil\_plant MD}}$ were found in F1P2, which was consistent with the smaller overall seasonal $K_{\text{soil\_plant}}$ (as the slope of the linear relationship between sap flow and the difference in effective soil water potential and sunlit leaf water potential) (see Fig. S7).

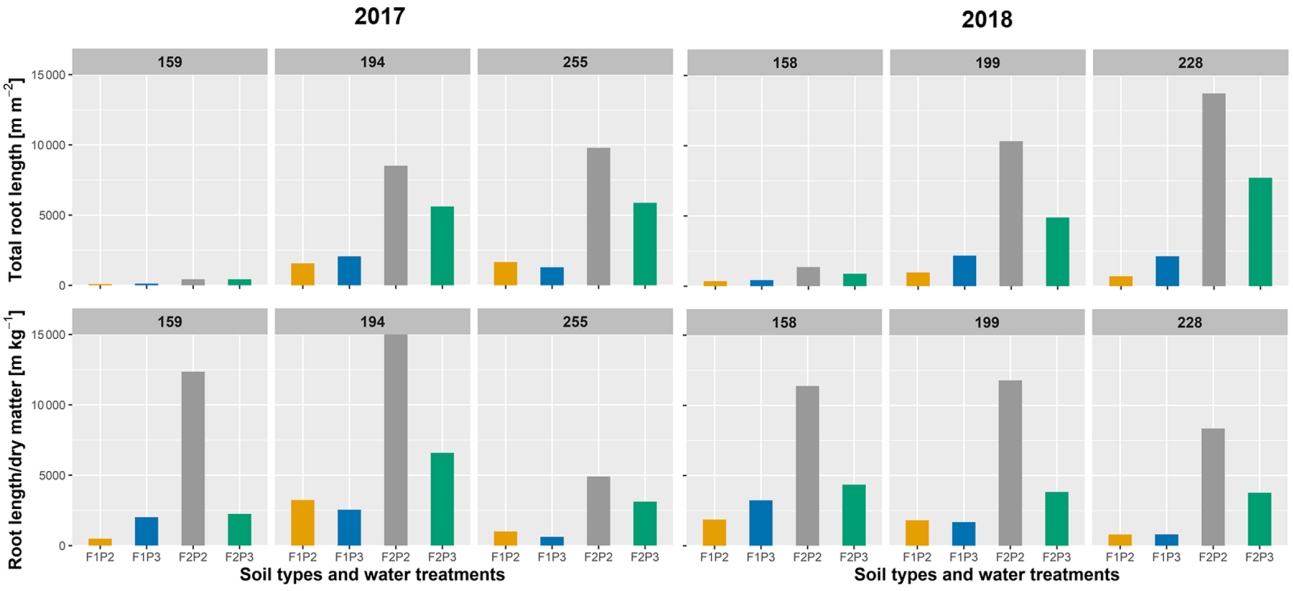


**Figure 3.** Observed root length from minirhizotubes (m m$^{-2}$) and ratio of root length per shoot dry matter (m kg$^{-1}$) from the rainfed (P2) and irrigated (P3) plots of the stony soil (F1) and silty soil (F2) in the two growing seasons (left panel) in 2017 and in 2018 (right panel). More specifically, 8 June (DOY 159), 13 July (DOY194), and 12 September (DOY 255) in 2017 are stem elongation, silking, and harvest, respectively; 7 June (DOY 158), 18 July (DOY 199), and 16 August (DOY 228) in 2018 are stem elongation, 1 week after silking, and 1 week before harvest, respectively (see also Fig. 2).

The $\psi_{\text{soil\_effec MD}}$ was substantially different in the two soil types and water treatments in 2018 (Fig. 7a). Both F1P2 and F1P3 showed a gradual drop in $\psi_{\text{soil\_effec MD}}$ from 15 June until the third week of July and then increased after irrigation events on 18 July (Fig. S2b). However, $\psi_{\text{soil\_effec MD}}$ of F1P2 was much lower than F1P3 toward the harvest. The $\psi_{\text{soil\_effec MD}}$ of F2P2 and F2P3 only decreased progressively from around 10 July till harvest even though there was water supply from the irrigation (Fig. S2b). The water applied by irrigation and coming in by rainfall was insufficient to wet up the deeper soil layers, which remained dry. The low $\text{Gs}_{\text{MD}}$ corresponded to the lowest $\psi_{\text{sunlitleaf MD}}$ and $K_{\text{soil\_plant MD}}$ from the F1P2 (Fig. 7c and d). The $K_{\text{soil\_plant MD}}$ from all plots was ranging from 0.12 to 0.91 mm h$^{-1}$ MPa$^{-1}$. There was the drop in $K_{\text{soil\_plant MD}}$ (i.e., 3–9 or 17–18 July) before irrigation in this plot. However, it increased after the irrigation (i.e., 10 and 19 July). This suggests that $K_{\text{soil\_plant}}$ depends strongly on the soil water content and the conductivity of the rhizosphere.

### 3.2.3 Relationships of stomatal conductance, transpiration, and photosynthesis with plant hydraulic variables at the plant canopy level

The slope of linear relationship between sap flow and difference in $\psi_{\text{soil\_effec}}$ and $\psi_{\text{sunlitleaf}}$ is shown for 3consecutive days (leaf water potential measurements from the predawn) and before and after irrigation application (17, 18, and 19 July 2018) (Fig. 8). On both 17 and 18 July, the difference between $\psi_{\text{soil\_effec}}$ and $\psi_{\text{sunlitleaf}}$ was around −1.6 MPa with very low transpiration rates in treatment F1P2, which was associated with very low plant hydraulic conductance and leaf curling. The whole-plant hydraulic conductance was disrupted on these 2 d (0.06 and 0.16 mm h$^{-1}$ MPa$^{-1}$ for 17 and 18 July, respectively). Water was supplied on 18 July at 13:00 for the irrigated plots (F1P3, F2P3) as well as for F1P2 at 16:00 (for saving the plant from death due to severe drought stress). $K_{\text{soil\_plant}}$ was slightly changed (0.43 and 0.57 mm h$^{-1}$ MPa$^{-1}$ for F1P3 on 18 and 19 July, respectively, and 0.5 and 0.58 mm h$^{-1}$ MPa$^{-1}$ for F2P3 on 18 and 19 July, respectively). However, the increase in $K_{\text{soil\_plant}}$ was substantial in the F1P2 after the irrigation. Soil water replenishment and an increase in the root–soil contact (Fig. 7a) allowed the $K_{\text{soil\_plant}}$ to recover overnight to 0.46 mm h$^{-1}$ MPa$^{-1}$. This resulted in a narrower water potential gradient between root zone and sunlit leaf and in a higher transpiration rate on 19 July.

Seasonal averages of different midday hydraulic conductance components (root system hydraulic conductance – $K_{\text{soil\_root}}$, stem hydraulic conductance – $K_{\text{stem}}$, and whole-plant hydraulic conductance – $K_{\text{soil\_plant}}$) are shown in Fig. 9. In the same year, the $K_{\text{stem}}$ was not much different among F1P3, F2P2, and F2P3 plots. The $K_{\text{stem}}$ of those plots was slightly higher than in F1P2 in both years. In general, the $K_{\text{soil\_root}}$ was lower than the $K_{\text{stem}}$. Overall, the estimated $K_{\text{soil\_plant}}$ was around $1/(1/K_{\text{soil\_root}} + 1/K_{\text{stem}})$ regardless of soil types, years, and water treatments. The $K_{\text{soil\_root}}$ and $K_{\text{soil\_plant}}$ in F1P2 in 2018 were much lower than the remain-

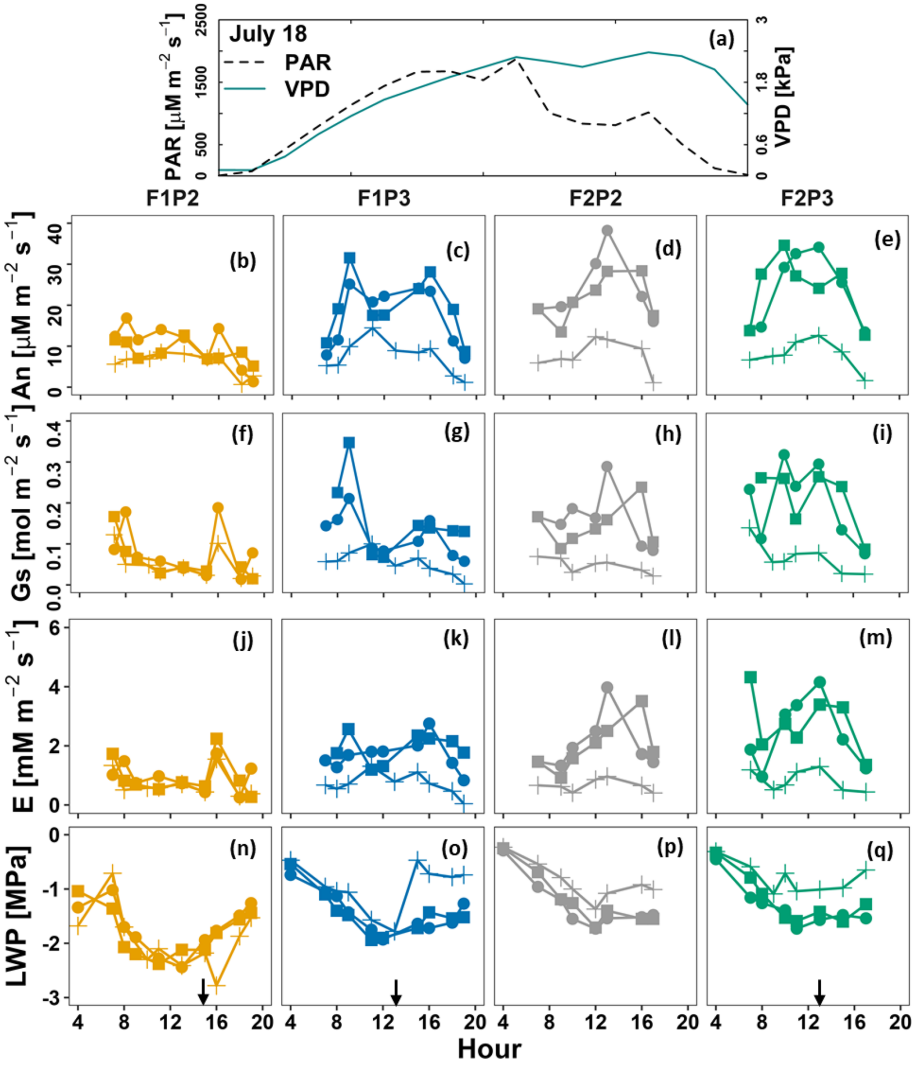


**Figure 4.** Diurnal course of **(a)** photosynthetically active radiation (PAR) and vapor pressure deficit (VPD), **(b–e)** leaf net photosynthesis (An), **(f–i)** leaf stomatal conductance (Gs), **(j–m)** leaf transpiration ($E$), and **(n–q)** leaf water potential (LWP) on 18 July in maize in 2018 before irrigation at the rainfed (P2) and irrigated (P3) plots of the stony soil (F1) and silty soil (F2). Measurement was carried out from a shaded leaf (plus symbol with line) and two sunlit leaves (solid dot – lines and solid square – lines). Crop was irrigated at 13:00, 13:00, and 16:00 for F1P3, F2P3, and F1P2, respectively (22.75 mm for each plot) (Fig. S2). Black arrows indicate time of irrigation.

ing plots, while the $K_{soil\_root}$ and $K_{soil\_plant}$ were not much different among plots in 2017. Our results indicated that there was an impact of the soil hydraulic conductance on $K_{soil\_root}$ and $K_{soil\_plant}$. Although there is a large difference in total root length between the two soil types (e.g., F1P3 versus F2P2 or F2P3 versus F2P2), $K_{soil\_root}$ and $K_{soil\_plant}$ in those two plots were not much different. This could be explained by the fact that $K_{soil\_plant}$ was not only dependent on root length but also dependent on the variability in root segment hydraulic conductance.

### 3.3 Relative importance of root and leaf area growth to transpiration and crop performance at canopy level

Drought stress was observed in the rainfed plot (F2P2) in the second week of June 2017 with mild leaf rolling. The crop then recovered due to sufficient rainfall and lower evaporative demand. Drought stress occurring again at the stem elongation phase caused reduction of plant size (height and stem diameter) (Fig. S6) as well as a slight reduction of leaf area and biomass in this plot (Fig. S3a, c). Transpiration per unit of leaf area did not differ much among water treatments and soil types in 2017 (Fig. S8). The opposite was the case for the transpiration rate per unit of root length. The observed root length at different soil depths (Fig. 2) and total root length for

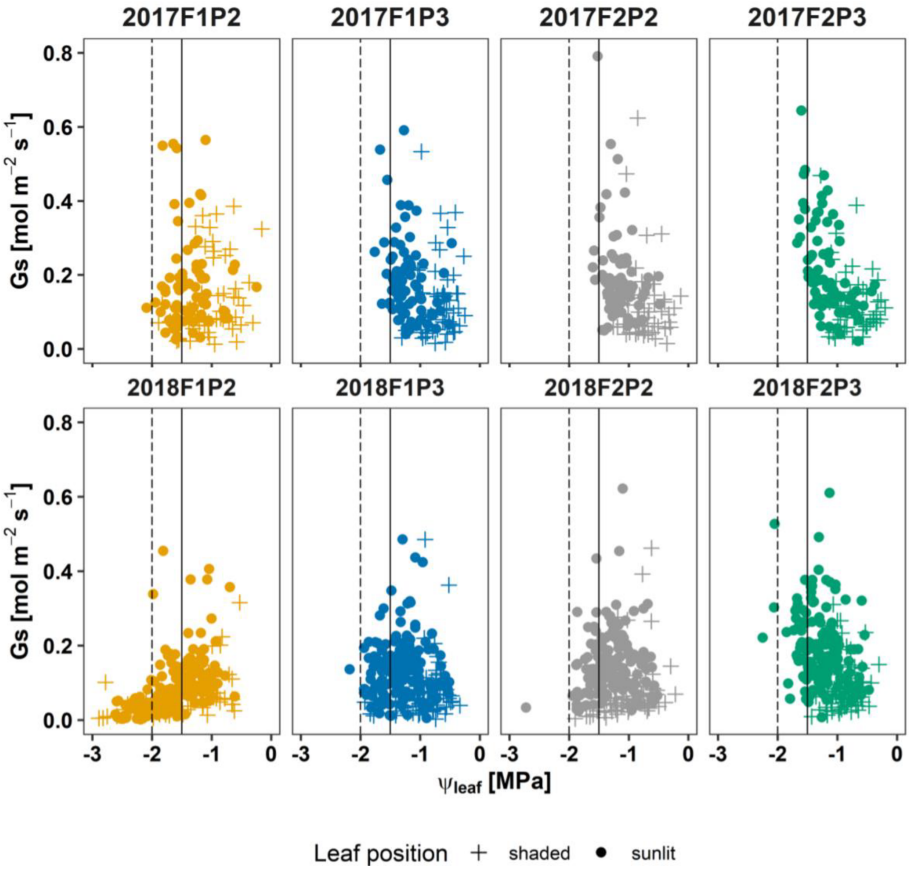


**Figure 5.** Seasonal stomatal conductance to water vapor (Gs) versus leaf water potential ($\psi_{leaf}$) in 2017 (top panel) and in 2018 (bottom panel) at the rainfed (P2) and irrigated (P3) plots of the stony soil (F1) and silty soil (F2). Vertically continuous and dashed lines indicated $\psi_{leaf}$ at −1.5 and −2 MPa, respectively. Measurement was carried out from a shaded leaf (plus symbol) and two sunlit leaves (solid dots).

two plots in the stony soil were much smaller than in the silty soil (Fig. 3). Therefore, transpiration per unit of root length in the stony soils (F1P2 and F1P3) was almost 3 times higher than transpiration in the silty soil. For the same soil, transpiration per unit root length of the irrigated treatment was slightly larger than in the rainfed plot.

The differences in sap flow per plant between water treatments and soil types were more pronounced in 2018 (Fig. S9). The highest transpiration rate was observed in the irrigated plots (F1P3 and F2P3), followed by the rainfed plot of the silty soil (F2P2), and it was the lowest in the rainfed plot of the stony soil (F1P2). These observations were in line with the differences in biomass and leaf area index between the treatments (Fig. S3b, d) and plant size (Fig. S6b–d). In 2018, severe leaf rolling was observed in the rainfed plot (F1P2) from the beginning of June until the end of the growing period in 2018 (Fig. S3d). Similar to 2017, transpiration per unit of root length was much higher in the stony plots than in silty plots. Also, for the silty soil, transpiration per unit of root length of the irrigated plot (F2P3) was higher than in the rainfed plot (F2P2).

Higher cumulative transpiration in the irrigated plots did not result in higher transpiration use efficiency (TUE) in both soil types (Fig. 10). For instance, TUE was 16.87 and 15.59 g mm$^{-1}$ for F1P2 and F2P2, respectively, while it was 15.47 and 14.79 g mm$^{-1}$ for F1P3 and F2P3, respectively, in 2017 (Fig. 10a). For the same soil, the rainfed plot showed slightly higher TUE than the irrigated plot. When comparing the TUE of maize of the two soil types for the same water treatment, TUE in the stony soil was almost the same in the silty soil. The TUE was not much different among treatments and soil types in 2018. Overall, TUE in 2017 was higher than in 2018 (Fig. 10b).

## 4 Discussions

### 4.1 Effects of soil types, water application, and climatic condition on root growth

Our root observations showed that soil type affected root growth more than water treatment (Fig. 2). Root growth was strongly inhibited by the stony soil where much lower root length was observed than in the silty soil, especially

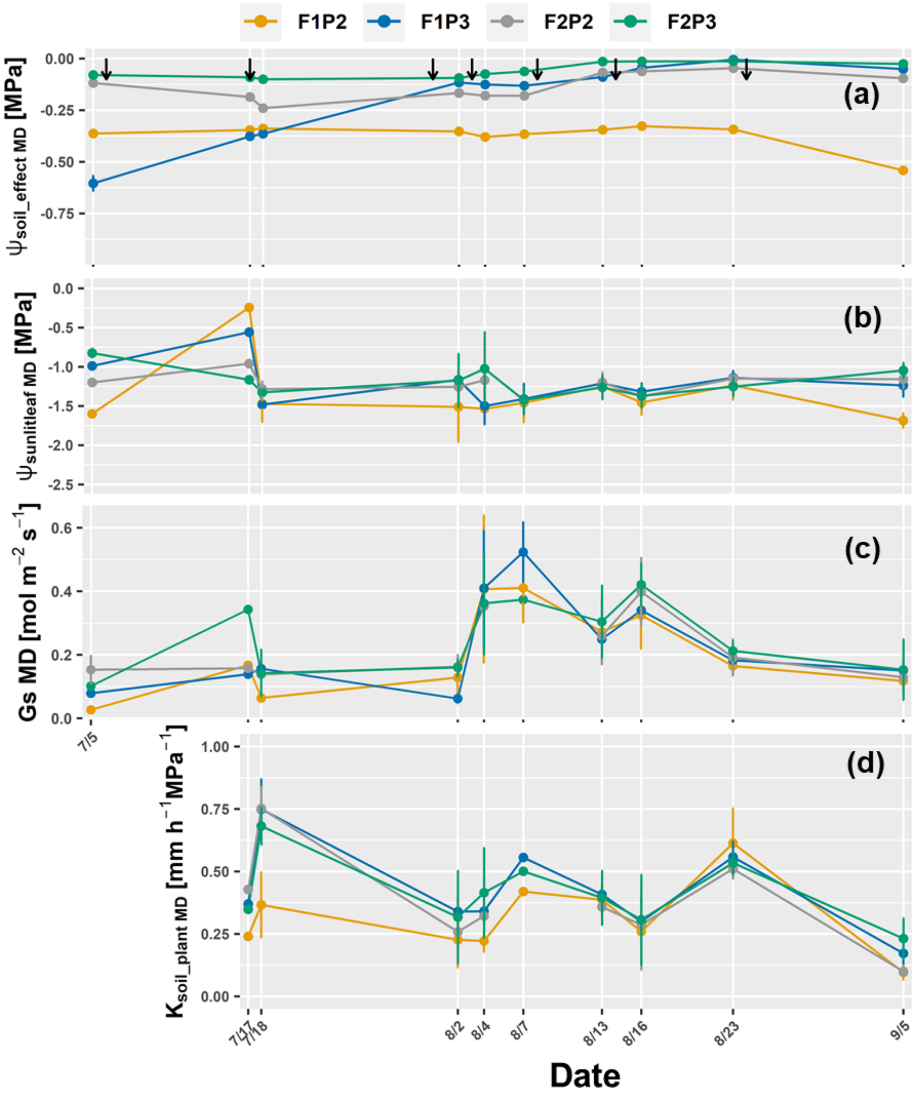


**Figure 6.** Dynamic of around midday (MD) of **(a)** the effective soil water potential ($\psi_{\text{soil\_effec MD}}$), **(b)** sunlit leaf water potential ($\psi_{\text{sunlitleaf MD}}$), **(c)** stomatal conductance (Gs MD), and **(d)** whole-soil–plant hydraulic conductance ($K_{\text{soil\_plant MD}}$) in the growing season 2017 from the rainfed (P2) and irrigated (P3) plots of the stony soil (F1) and silty soil (F2). Error bars indicate the standard deviation of the different values taken around midday (11:00, 12:00, 13:00, and 14:00) of different sunlit leaves. Whole-soil–plant hydraulic conductance is shown from 17 July when sap flow was measured. The black arrows indicate the irrigation events for the irrigated treatments F1P3 and F2P3 in the showing period.

in the deeper soil layers. This was consistent with the findings reported in Morandage et al. (2021), where a linear increase in stone content resulted in a linear decrease in rooting depth across all stone contents and developmental stages. Also, both simulations and observations indicated that rooting depth increased due to the presence of cracks in the lower minirhizotron facility (Morandage et al., 2021), which could explain the high root length between 40 and 120 cm soil depths, which was observed in the silty soil in both years.

In terms of the ratios of root length to shoot biomass, Ordóñez et al. (2020) reported much larger figures of for instance 880 cm $g^{-1}$ in different locations and under different N application rates in maize growing in the Midwest United States. Jorda et al. (2022) reported a wide range of ratios of root length to shoot biomass from 200 to 1000 cm $g^{-1}$ around flowering time of maize, depending on the wild type and root hair mutant genotypes growing on either loamy or sandy soils. More roots and higher ratios of root length to shoot biomass were found in the sand than in the loam in both wild type and root hair mutant genotypes (Jorda et al., 2022; Vetterlein et al., 2022). Cai et al. (2018) observed much larger ratios of root length to shoot biomass in drought-stressed plots than in irrigated plots in both soil types in winter wheat, which indicated the alternation of sink–source relationships

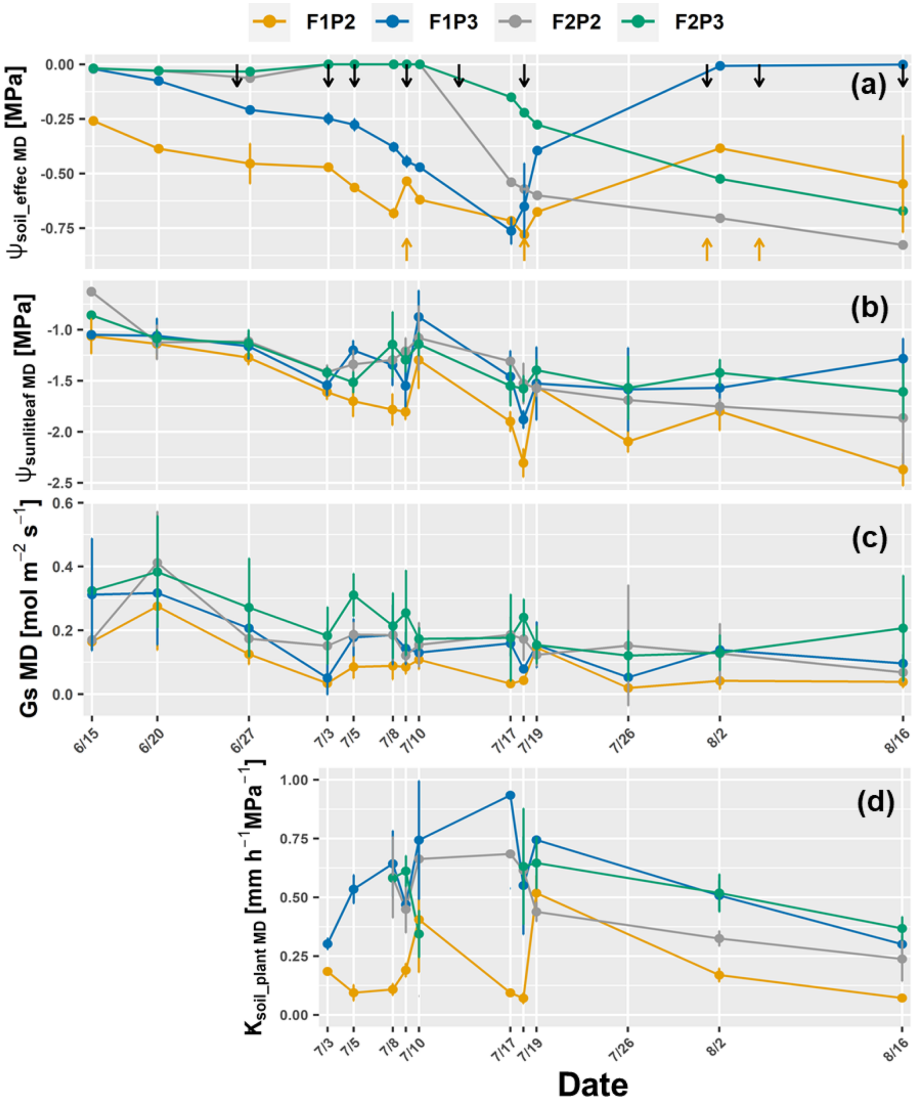


**Figure 7.** Dynamic of around midday (MD) of **(a)** the effective soil water potential ($\psi_{\text{soil\_effec MD}}$), **(b)** sunlit leaf water potential ($\psi_{\text{sunlitleaf MD}}$), **(c)** stomatal conductance (Gs MD), and **(d)** whole-soil–plant hydraulic conductance ($K_{\text{soil\_plant MD}}$) in the growing season 2018 from the rainfed (P2) and irrigated (P3) plots of the stony soil (F1) and silty soil (F2). Error bars indicate the standard deviation of the different values taken around midday (11:00, 12:00, 13:00, and 14:00). Leaf water potential and stomatal conductance were two sunlit leaves and one shaded leaf at each measured hour. Whole-soil–plant hydraulic conductance is shown from 3 July when sap flow was measured. The black arrows indicate the irrigation events for the irrigated treatments F1P3 and F2P3, while the orange arrow indicates the irrigation application for the rainfed plot in the stony soil (F1P2).

to cope with water stress. This study emphasized that more assimilates are used to promote root growth and extract more water under drought stress. However, this was not the case for the stony soil in our work where the drought stress was more pronounced, especially in 2018. A drop in soil water potential (Fig. S2b), and thus effective soil water potential (Fig. 6a), was substantial from 10 July 2018 to the harvest in the rainfed plot in the silty soil (F2P2), which was consistent with the reduction of leaf water potential (Fig. 6b), leaf area (Fig. S3c), total dry matter (Fig. S3d), and crop height (Fig. S6b) compared to the irrigated plot (F2P3). This indicates a mild water stress in 2018 in the rainfed plots in the silty soil. The larger ratios of root length to shoot biomass in this F2P2 plot in 2018 than in F2P3 could be explained by the change in source–sink relations where more assimilates were devoted to root growth, even at a later growth stage. Moreover, the low stone content and soil cracks (Morandage et al., 2021) might favor root growth in the deeper soil layers which are close to the shallow soil water table in the rhizotron facility with silty soil (Vanderborght et al., 2010). In conclusion, both soil texture and water conditions influenced

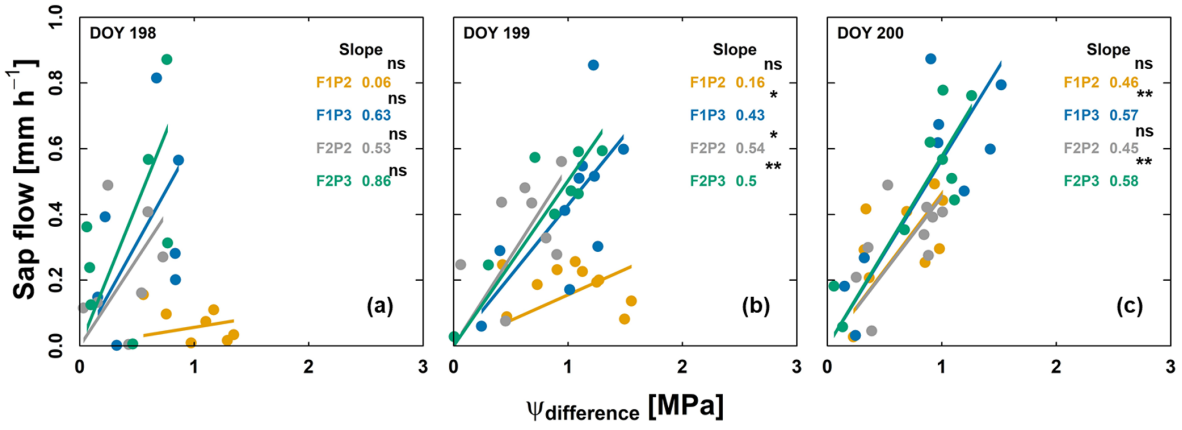


**Figure 8.** Relationship between sap flow and difference in effective soil water potential and sunlit leaf water potential ($\psi_{difference}$) from the rainfed (P2) and irrigated (P3) plots of the stony soil (F1) and silty soil (F2) on 3 consecutive measurement days from predawn in 2018: **(a)** 17 July – DOY 198, **(b)** 18 July – DOY 199, and **(c)** 19 July – DOY 200. Crop was irrigated on 18 July (DOY 199) at 13:00, 13:00, and 16:00 for F1P3, F2P3, and F1P2, respectively (22.75 mm for each plot). The unit of slope in the linear regression (or soil–plant hydraulic conductance) is mm $h^{-1}$ $MPa^{-1}$. Regression was based on the DEMING approach. The asterisks next to the slopes indicate a significant correlation between two variables according to Pearson's method. ns denotes nonsignificant. * $p < 0.05$. ** $p < 0.01$. *** $p < 0.001$.

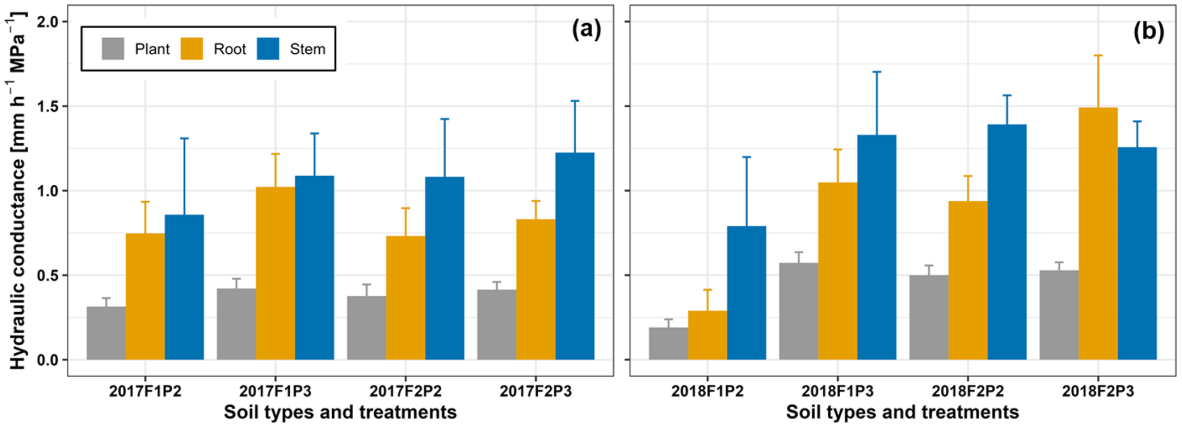


**Figure 9.** Comparison of different midday hydraulic components (mm $h^{-1}$ $MPa^{-1}$): soil–plant (grey bars), soil–root (yellow bars), and stem (blue bars) from the rainfed (P2) and irrigated (P3) plots of the stony soil (F1) and silty soil (F2) in the two growing seasons **(a)** in 2017 and **(b)** in 2018. The error bars indicate the standard deviation from measurements around midday (11:00, 12:00, 13:00, and 14:00) on different measured days in 2017 (with $n = 4 \times 9$ d; Figs. S10, S11, and 6) and in 2018 (with $n = 4 \times 10$ d; Figs. S10, S12, and 7).

the root growth; however, the effects of the former on root length were more pronounced than those of the latter.

In the stony soil, which has a considerably smaller water-holding capacity than the silty soil, root length was considerably smaller than in the silty soil. Nevertheless, water uptake per unit root length was much larger than in the fine soil. This also means that the hydraulic conductance per unit root length must have been much larger in the stony soil than in the fine soil. Cai et al. (2018) observed a similar effect for winter wheat, but they found much smaller differences in the root-length-normalized root conductance. The higher root-length-normalized root conductance means that the anatomy of the root tissues must have been influenced by the soil texture and compensated the considerably smaller root length in the stony soil. Looking at the effect of water treatments in the silt soil, the nonirrigated plot had more roots than the irrigated one, and both had more roots in the year with high VPD. But the soil–root conductance was higher in the irrigated plot than in the rainfed plot. This means that in the irrigated plot, the soil–root conductance per unit root length was higher than in the rainfed plot. This could either be due to wetter soil conditions and higher soil conductance or be due to a larger conductance of the root tissues. Especially in 2017 when the silty soil was wetter, the slightly larger soil–root conductance in the irrigated plot is most likely the result of larger root tissue conductance in the irrigated plot. Thus, how root architecture (here represented simply by the total root length) and root tissue conductivities "respond" to

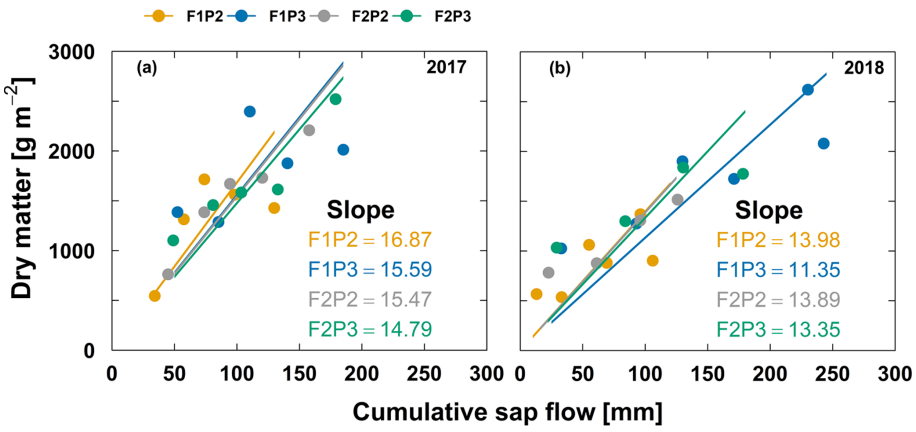


**Figure 10.** Relationship between aboveground dry matter and cumulative sap flow from the rainfed (P2) and irrigated (P3) plots of the stony soil (F1) and silty soil (F2) in the two growing seasons in **(a)** 2017 and **(b)** 2018. The unit of slope linear relationship is g mm$^{-1}$. The lower number of data points in **(b)** in 2018 from the F2P2 and F2P3 plots was due to the missing values for measured sap flow because of sensor disconnection. For aboveground dry matter, each point represents the average of two sampling replicates, except the harvest with five sampling replicates.

drought stress might be opposite, depending on the comparisons that are made. When the stony soil and silt soil are compared, the higher "stress" due to lower water availability in the stony soil resulted in fewer roots with a higher root tissue conductance in the soil with more stress. When comparing the rainfed with the irrigated plot in the silty soil, the higher stress in the rainfed soil resulted in more roots with a lower root tissue conductance in the treatment with more stress. This indicates that the response to water stress can be different depending on soil conditions or water treatments.

### 4.2 Effects of soil types, water application, and climatic condition on stomatal conductance, photosynthesis, transpiration, leaf water potential, and plant hydraulic conductance

#### 4.2.1 Leaf water potential and stomatal conductance as affected by soil water conditions

In previous work, Koehler et al. (2022) reported that maize stomata closed at lower negative leaf water potentials in sand than in loam growing under a controlled environment. Cai et al. (2022b) investigated transpiration response of pot-grown maize in two contrasting soil textures (sand and loam) and exposed to two consecutive VPD levels (1.8 and 2.8 kPa). Transpiration rate decreased at less negative soil matric potential in sand than in loam at both VPD levels. In sand, high VPD generated a steeper drop in stomatal conductance with decreasing leaf water potential, which indicated that the transpiration and stomatal responses depend on soil hydraulics. In our study, stomata closed earlier and at more negative soil and leaf water potentials in the stony soil than in the silty soil (see Figs. 4, 7, S4, S5). The lower soil-water-holding capacity of the stony soil compared to the silty soil resulted in lower soil water potential and smaller total plant hydraulic conductance, which in turn led to earlier stomatal closure and to more negative soil water potential in the stony soil.

Stomatal control is an early and effective response to water stress to prevent the plant from water loss and dehydration. Maize is considered an isohydric plant which closes its stomata to maintain leaf water potential above critical levels (Tardieu and Simonneau, 1998). Our results showed that minimum leaf water potential varied among treatments ($-1.5$ MPa for F1P3, F2P2, and F2P3 and up to $-2$ MPa for F1P2 in 2017, while in 2018 minimum values were $-2$ MPa for F2P3, F2P2, and F2P3 and $-2.7$ MPa for F1P2) (Figs. 5, 6, and 7). In conclusion, our results confirmed that the minimum $\psi_{leaf}$ not only depended on genotypic differences but also was influenced by soil types, soil hydraulic conductance, and atmospheric demand.

#### 4.2.2 Hydraulic conductance components as affected by soil water conditions

Estimates of hydraulic components in soil–plant–atmosphere continuum are important not only to understand its underlying relationship to other crop characteristics (stomatal conductance, transpiration, and photosynthesis) but also to provide modeling parameters in process-based soil–root–shoot models (Nguyen et al., 2020; Sulis et al., 2019; Nguyen et al., 2022b). Measurement of the components of hydraulic conductance are challenging under field conditions because it requires the estimation of transpiration and root to leaf water potential gradients. To our knowledge, our results were unique with regards to the dynamics of $K_{soil\_plant}$ for field-grown maize on two soil types and under contrasting water and climatic conditions. Our seasonal $K_{soil\_plant}$ ranged from 0.12 to 0.9 mm h$^{-1}$ MPa$^{-1}$ (Figs. 6, 7, 8, and S7). Root system hydraulic conductance

ranged from 0.26 to 1.47 mm $h^{-1}$ $MPa^{-1}$ (Fig. 9). Note that the unit of $K_{soil\_plant}$ as mm $h^{-1}$ $MPa^{-1}$ could be equivalent to the unit of $10^{-5}$ $h^{-1}$ if one assumes 1 MPa is approximately $10^5$ mm in terms of pressure head. Cai et al. (2018) reported root hydraulic conductance in winter wheat from 0.05 to 0.5 mm $h^{-1}$ $MPa^{-1}$ in two similar soil types. Nguyen et al. (2020) also reported $K_{soil\_plant}$ in winter wheat from 0.0625 to 0.461 mm $h^{-1}$ $MPa^{-1}$. Meunier et al. (2018) focused on estimating the root system hydraulic conductance of maize in a container experiment where the range of $K_{soil\_plant}$ was much larger from 0.37 to 36 mm $h^{-1}$ $MPa^{-1}$ for the plant density of 10 plants per square meter. Jorda et al. (2022) estimated root system hydraulic conductance of 0.5 to $1.5 \times 10^{-3}$ $d^{-1}$, which would be roughly between 2 and 6 mm $h^{-1}$ $MPa^{-1}$. In our work, except the F2P2 in 2018, the stem hydraulic conductance was 10 % to 60 % higher than root system hydraulic conductance. Gallardo et al. (1996) reported that stem hydraulic conductance of wheat was lower than root system conductance at around 71 to 91 d after sowing (DAS), but they were similar at 102 DAS. In lupine, stem hydraulic conductance was 2 times higher than root system conductance regardless of measured days. The larger root length in wheat than lupine did not necessarily result in higher root conductance in wheat. Together with this study, our study emphasizes the values of stem hydraulic conductance compared to the root hydraulic conductance in maintaining water potential gradient from shaded leaf or plant color to the sunlit leaf.

Our results showed clear differences in $K_{soil\_plant}$ among treatments where a much lower $K_{soil\_plant}$ was observed in F1P2 than in F2P2 (see Fig. 8 for 2018; Figs. 6, 7 and S7 for both years). This indicated the soil texture dependence for whole-plant hydraulic conductance. Maize plants with shorter root systems (i.e., rainfed plot in the stony soil in 2018) (Fig. 3) had lower plant hydraulic conductance. Our results indicated that there was an impact of soil hydraulic conditions on $K_{soil\_plant}$ via the reduction of root system hydraulic conductance. Our analysis for 3 consecutive measurement days in 2018 (Fig. 8) showed that in the silty soil, $K_{soil\_plant}$ decreases when soil water potentials become more negative. For instance, in the silty soil in 2018 when the soil water potentials were considerably lower in the rainfed than in the irrigated plot (e.g., after 10 July), $K_{soil\_plant}$ was lower in the rainfed than in the irrigated plot. In the stony soil, the $K_{soil\_plant}$ and leaf water potentials seem to decrease more considerably (compared to the silty soil) when the soil water potentials become more negative. In other words, $K_{soil\_plant}$ increased considerably when the soil water potentials in the stony soil increased. In our work, $K_{soil\_plant}$ increased slowly after irrigation mainly for the severe-water-stress plot (see F1P2 on 19 July in Figs. 7d and 8c). This implied that added soil water by irrigation took some time to recover the soil–root contact within the rhizosphere.

#### 4.2.3 Relationships of stomatal conductance, transpiration, and photosynthesis with plant hydraulic variables

The transpiration rate and $K_{soil\_plant}$ (slope of linear regression lines in Fig. 8a and b) were very low in the rainfed plot under the stony soil (F1P2), which was associated with the large $\psi_{difference}$ (Fig. 8a, b) and the lower stomatal conductance compared to other plots (Fig. 7c). The $K_{soil\_plant}$ slightly increased after irrigation (18 July – DOY 199 in Fig. 8b), corresponding with the smaller $\psi_{difference}$ (Fig. 8b) and an increase in stomatal conductance (Fig. 7c). Seasonal $K_{soil\_plant}$ was low in the rainfed plot under stony soil (F1P2) with the larger $\psi_{difference}$ (Fig. S7). In addition, our study showed that the midday stomatal conductance, photosynthesis, and transpiration were significantly correlated only with midday $K_{soil\_plant}$ in the rainfed plot in the stony soil (F1P2) in 2018 where high VPD and temperature occurred (Table S1 and Figs. S10 and S11 in the Supplement). Maize plants had lower plant hydraulic conductance and more negative soil water potential in the rainfed plot in the stony soil, and they exhibited earlier stomatal closure compared to the same plot in the silty soil. This was in line with a study by Abdalla et al. (2022) which suggested that, during soil drying, stomatal regulation of tomato is controlled by root and soil hydraulic conductance. Recent work by Müllers et al. (2022) on fava bean and maize suggested that differences in the stomatal sensitivity among plant species can be partly explained by the sensitivity of soil–plant hydraulic conductance to soil drying. The loss of conductance has immediate consequences for leaf water potential and the associated stomatal regulation. Cai et al. (2022b) also showed that the decrease in sunlit leaf stomatal conductance was well correlated with the drop in soil–plant hydraulic conductance, which was significantly affected by soil texture. This was confirmed in our work where the stony soil strongly impacted on root growth, modulated $K_{soil\_plant}$, and consequently influenced the leaf stomatal conductance, photosynthesis, and transpiration.

### 4.3 Relative contribution of water control by leaves and roots on transpiration and transpiration use efficiency

Responses of crops via stomatal control to reduce water loss at leaf scale while maintaining leaf photosynthesis and water use efficiency were reported earlier (Nguyen et al., 2022a; Vitale et al., 2007). In addition to that, in the maize experiments in 2017 and 2018, leaf rolling was observed in both rainfed plots in the stony and the silty soil in the second week of June 2017 and from the beginning of June until the end of the growing period in 2018. This indicates another dehydration avoidance mechanism resulting from morphological adjustments, which is an effective strategy for leaf senescence (Aparicio-Tejo and Boyer, 1983; Richards et al., 2002). Stomatal closure resulted in a larger reduction of tran-

spiration and assimilation in the rainfed plots than in irrigated plots with the same soil type (Figs. 4, 5, S4, S5, and S9a). There was reduction of shoot biomass (also stem size and leaf size adjustments) in F1P2 compared to other plots. However, the TUE was not smaller in this plot than the remaining plots. These observations confirm that plant size adjustments through reduction of height, leaf width, and length are efficient responses to reduce water loss at canopy scale in addition to stomatal control at the leaf level.

Relative contribution of leaf area to transpiration has been highlighted in wheat where reduction of tiller number resulted in significantly lower leaf area index (LAI), thus lower canopy transpiration (Cai et al., 2018; Trillo and Fernández, 2005; Nguyen et al., 2022a). However, root system conductance per unit of leaf area and per unit root mass was strongly reduced and eventually more than reduction of leaf area under water stress (Trillo and Fernández, 2005). In our work, expressing the transpiration per unit of root length on the one hand allowed us to analyze the role of total root length to water uptake. However, on the other hand, the lower total root length did not necessarily result in a lower root water uptake and vice versa. For instance, the rainfed plot of the treatment F2P2 had the larger total root length, which could postpone the effect of soil water limitations in drying soils due to greater ability to extract water from subsoils. Therefore, transpiration was very similar between F2P2 and F2P3. Despite the much lower total root length in the stony soil, $K_{\text{soil\_plant}}$ in the irrigated plot (F1P3) was not much lower than in the same water treatment in the silty soil (F2P3; Figs. 6d, 7d, 8, and S7). This could be explained by the fact that the $K_{\text{soil\_plant}}$ variability not only depended on root architecture (here the root length and distribution) but also depended on the variability in root segment hydraulic properties, which has also been illustrated and discussed in Zwieniecki et al. (2002), Frensch and Steudle (1989), Meunier et al. (2018), Couvreur et al. (2014), and Ahmed et al. (2018). Moreover, the contribution of shoot hydraulic conductance could be large in plants (Gallardo et al., 1996; Trillo and Fernández, 2005; Sunita et al., 2014), which also confirmed in our work. In our work, $K_{\text{soil\_plant}}$ comprised root and shoot conductance, which are directly influenced by soil hydraulics. Our estimates of $K_{\text{soil\_plant}}$ varied with transpiration and gradients of $\psi_{\text{sunlitleaf}}$ and $\psi_{\text{soil\_effec}}$. Thus, any change in soil hydraulic conductance will change the root to shoot water potential. Consequently, it will affect the gradients between the shoot and root rhizosphere (Carminati and Javaux, 2020). Thus, our study reveals the importance of both soil texture characteristics and root phenotypic traits (here root length) in regulating plant transpiration (Cai et al., 2022a). Despite lower root length in the stony irrigated plot, transpiration rate was not much lower than in the silty irrigated plot in our work. This could be related to another property of the root, such as root segment conductance or other root traits (e.g., root hair). Further investigation with extensive measurements of roots including axial and radial root conductance at field scale will be required to better explain the observed results. Other traits like root hair density (Cai et al., 2022a) or higher root length density (Vadez, 2014) could contribute to the soil to root water potential and root-zone hydraulic conductance where dense root hairs delay soil water deficit in drying soils. However, contrasting results have shown that root hairs did not have an effect on root water uptake (see Jorda et al., 2022). The role of root hairs could not be analyzed in our work, which was based on root data from minirhizotron images.

This study investigated soil–water–plant relations, more specifically the interactions between the root and shoot growth processes and water fluxes under variations of soil water status and atmospheric demands. To the best of our knowledge, the comprehensive data collected from soil to root, plant, and atmosphere under field conditions in this work were unique. However, we acknowledge the lack of treatment replicates, which was due to the complex and expensive construction of the rhizotron facilities. We also acknowledge the small size of plots that did not allow the extensive destructive sampling (i.e., leaf area, biomass, or determination of leaf water potential). Each rhizotron site originally contained the irrigated, rainfed, and rainout sheltered plots (Nguyen et al., 2022a; Cai et al., 2016). The overall aim of the experiments was to investigate the root and shoot responses and gas fluxes ($CO_2$ and $H_2O$) of wheat and maize to the variations of soil water and soil hydraulics. Note that the studies did not intend to investigate the impacts of similar irrigation strategies on plant water status among seasons (i.e., in 2017 and 2018) because the irrigation practices were less common in the regions. The collapse of manual rainout shelters due to strong wind after the 2016 growing season resulted in only two water treatments (rainfed and irrigated). Based on experiences from the previous seasons (wheat), we argued that such combinations of two water treatments and two soil types, to some extent, could still create a wide range of soil water conditions for the maize trial. For instance, the "rainfed" treatment on the stony soil in the upper rhizotron (F1P2) could lead to severe water stress compared to other treatments, especially in the summertime when the atmospheric evaporative demand is high. In fact, mild water stress was observed at F1P2 around mid-June in 2017. In 2018, the sites were slightly modified to induce more severe water stress (Nguyen et al., 2022a). One rainfed plot with stony soil had late sowing, while one rainfed plot with silty soil had a higher sowing density (data not shown in the study). Unprecedented weather (extremely hot and dry) in 2018 resulted in severe drought stress at the rainfed plots with stony soil. To compare the effects of soil types and water treatments on the crop, we present here only data from two plots (rainfed and irrigated) for two soil types. In spite of the experimental limitations, the relative differences among the treatments, soil types, and seasons, as well as measured dates, are clearly illustrated, which ultimately supported the overall aim of our study.

The simultaneous measurements of atmospheric conditions, leaf water potential, and transpiration rates (coupled with measurements of root, stem, and whole-soil–plant hydraulic conductance, root architecture (root length), and soil water potential distribution) illustrate the complex responses of the shoot and root growth and hydraulic conductance vulnerability to soil water availability. The different responses of crop processes to soil hydraulics and climatic conditions suggest further field investigations for other soil types, growing seasons, and water regimes. Future studies considering the effects of progressive soil drying or irrigation strategies on plant water status and crop growth at field conditions will be necessary. This is very relevant for those crop-growing regions that require irrigation. Our results show that the leaf water potential threshold can vary within the same genotype depending on soil types, climatic conditions, and water management. Large variability in minimum leaf water potential has been reported for maize genotypes under greenhouse conditions (Welcker et al., 2011). Field studies are required concerning the stomatal functions, water relations, hydraulic vulnerability traits, and root : shoot responses, especially of different maize cultivars in responding to drought stress. This will suggest implications for selecting agronomic cultivars and traits under changing climates. Results from this study show that soil–crop models should not only focus on simulating stomatal regulations to capture the response to drought stress but also require adequate representations of root and leaf growth and adjustments. The soil hydraulics strongly influenced soil water availability and crop growth. Regional application of soil–crop models for simulating gas fluxes and crop growth processes and for estimating irrigation amounts must account for the environmental heterogeneity within the spatial simulation unit, whereas the soil heterogeneity is the key variable.

## 5 Conclusion

We presented plant hydraulic characteristics and crop growth from root to shoot of maize under field-grown conditions with two soil types (silty and stony), each soil with two water regimes (irrigated and rainfed) for two growing seasons (2017 and 2018). Our results confirmed that root length and ratios of root length to shoot biomass were modulated by soil types and water treatment but less by seasonal evaporative demand. An increase in the ratio of root length to shoot biomass was an important response of maize that allows plants to extract more water under drought stress, which occurred more in the silty soil and less in the stony soil due to the higher content of stony material.

Another conclusion is that stomatal regulation maintains leaf water potential at certain thresholds, which depends on soil types, soil water availability, and seasonal atmospheric demand. The stomata conductance was smaller and decreased at more negative leaf water potentials in the stony soil than in the silty soil. The leaf water potentials are affected by the soil–plant hydraulic conductance. In addition to stomatal regulation, leaf growth and plant size adjustments are important to regulate the transpiration and water use efficiency in the same year.

The lowest soil–plant hydraulic conductance was observed in the stony soil with severe drought stress compared to the silty soil, while its variation also depends on the soil water variation (before and after irrigation). Root system and soil–plant hydraulic conductance depended strongly on soil hydraulic properties. The "response" to stress can be completely opposite depending on the conditions or treatments that lead to the differences in stress that are compared. Therefore, it cannot be the "stress" alone that defines how a plant will react and adapt its root system. Modeling the impact of stress and the feedback between drought stress and plant development is likely controlled by properties or parameters that change with changing soil water availability and atmospheric water demand other than the plant stress level.

## Appendix A: Abbreviations

| | |
|---|---|
| DOY | day of the year |
| DAS | day after sowing |
| TUE | transpiration use efficiency |
| SF | sap flow |
| LAI | green leaf area index |
| PAR | photosynthetically active radiation |
| VPD | vapor pressure deficit |
| An | net leaf photosynthesis |
| $E$ | leaf transpiration |
| $\psi_{\text{leaf}}$ | leaf water potential |
| $\psi_{\text{sunlitleaf}}$ | leaf water potential of sunlit leaf |
| $\psi_{\text{shadedleaf}}$ | leaf water potential of shaded leaf |
| $K_{\text{soil}}$ | hydraulic conductance of soil |
| $K_{\text{root}}$ | root hydraulic conductance |
| $K_{\text{stem}}$ | stem hydraulic conductance |
| $\psi_{\text{soil\_effec}}$ | effective soil water potential |
| $\psi_{\text{difference}}$ | difference between effective soil water potential and sunlit leaf water potential |
| $K_{\text{soil\_root}}$ | root system hydraulic conductance (includes soil and root hydraulic conductance) |
| $K_{\text{soil\_plant}}$ | whole-plant hydraulic conductance (includes below- and aboveground components). |

*Data availability.* The meteorological data were collected from a weather station in Selhausen (Germany), which belongs to the TERENO network of terrestrial observatories. Weather data are freely available from the TERENO data portal (https://www.tereno.net/ddp/dispatch?searchparams=freetext-Selhausen, TERENO, 2020). The data which were obtained from the minirhizotron facilities are publicly available, specifically under-ground

data in Lärm et al. (2023, https://doi.org/10.1038/s41597-023-02570-9) and above-ground data in Nguyen et al. (2024, https://doi.org/10.34731/1a9s-ax66).

*Supplement.* The supplement related to this article is available online at: https://doi.org/10.5194/bg-21-5495-2024-supplement.

*Author contributions.* THN, TG, JV, and FE: conceptualization; THN, and HuH: data curation and data quality check (above-ground measurements); LL, FB, AK, JV, and AS: data curation and data quality check (belowground measurements); THN: formal data analysis and visualization; TG, JV, AS, and FE: funding acquisition and project administration; THN: writing (original draft); all authors: reviewing, editing, and finalizing the manuscript.

*Competing interests.* The contact author has declared that none of the authors has any competing interests.

*Disclaimer.* Publisher's note: Copernicus Publications remains neutral with regard to jurisdictional claims made in the text, published maps, institutional affiliations, or any other geographical representation in this paper. While Copernicus Publications makes every effort to include appropriate place names, the final responsibility lies with the authors.

*Special issue statement.* This article is part of the special issue "Drought, society, and ecosystems (NHESS/BG/GC/HESS inter-journal SI)". It is not associated with a conference.

*Acknowledgements.* We thank Matthias Langensiepen for his support and technical help in the TR32 project. We would like to thank all the student assistants and technicians for their considerable efforts in collecting the data in the field and the laboratories. We thank Jos van Dam, an anonymous reviewer, and the handling associate editor for their helpful and constructive comments on improving the manuscript.

*Financial support.* This work has partially been funded by Federal Ministry of Education and Research (BMBF) through the European SUSCAP project (grant no. 031B0170B) and COINS project (grant no. 01LL2204C) and the Deutsche Forschungsgemeinschaft (DFG, German Research Foundation) under Germany's Excellence Strategy (grand no. EXC 2070 390732324). We acknowledge the support of the SFB/TR32 "Pattern in Soil–Vegetation–Atmosphere Systems: Monitoring, Modelling, and Data Assimilation" funded by the Deutsche Forschungsgemeinschaft (DFG). Thuy Huu Nguyen and Thomas Gaiser also thank the DETECT/CRC 1502 research program, which is funded by the DFG (grant no. SFB 1502/1-2022, project no. 450058266).

*Review statement.* This paper was edited by Giulia Vico and reviewed by Jos C. van Dam and one anonymous referee.

## References

Abdalla, M., Carminati, A., Cai, G., Javaux, M., and Ahmed, M. A.: Stomatal closure of tomato under drought is driven by an increase in soil-root hydraulic resistance, Plant. Cell Environ., 44, 425–431, https://doi.org/10.1111/pce.13939, 2021.

Abdalla, M., Ahmed, M. A., Cai, G., Wankmüller, F., Schwartz, N., Litig, O., Javaux, M., and Carminati, A.: Stomatal closure during water deficit is controlled by below-ground hydraulics, Ann. Bot., 129, 161–170, https://doi.org/10.1093/aob/mcab141, 2022.

Ahmed, M. A., Zarebanadkouki, M., Meunier, F., Javaux, M., Kaestner, A., and Carminati, A.: Root type matters: Measurement of water uptake by seminal, crown, and lateral roots in maize, J. Exp. Bot., 69, 1199–1206, https://doi.org/10.1093/jxb/erx439, 2018.

Allen, R. G., Pereira, L. S., Raes, D., and Smith, M.: Crop evapotranspiration-guidelines for computing crop water requirements, FAO Irrig. Drain. Pap. No. 56, https://doi.org/10.1016/S0141-1187(05)80058-6, 1998.

Aparicio-Tejo, P. and Boyer, J. S.: Significance of Accelerated Leaf Senescence at Low Water Potentials for Water Loss and Grain Yield in Maize1, Crop Sci., 23, 1198–1202, https://doi.org/10.2135/cropsci1983.0011183X002300060040x, 1983.

Bauer, F. M., Lärm, L., Morandage, S., Lobet, G., Vanderborght, J., Vereecken, H., and Schnepf, A.: Combining deep learning and automated feature extraction to analyze minirhizotron images: development and validation of a new pipeline, bioRxiv [preprint], https://doi.org/10.1101/2021.12.01.470811, 2021.

Bourbia, I., Pritzkow, C., and Brodribb, T. J.: Herb and conifer roots show similar high sensitivity to water deficit, Plant Physiol., 186, 1908–1918, https://doi.org/10.1093/plphys/kiab207, 2021.

Cai, G., Vanderborght, J., Klotzsche, A., van der Kruk, J., Neumann, J., Hermes, N., and Vereecken, H.: Construction of Minirhizotron Facilities for Investigating Root Zone Processes, Vadose Zone J., 15, 1–13, https://doi.org/10.2136/vzj2016.05.0043, 2016.

Cai, G., Vanderborght, J., Couvreur, V., Mboh, C. M., and Vereecken, H.: Parameterization of Root Water Uptake Models Considering Dynamic Root Distributions and Water Uptake Compensation, Vadose Zone J., 17, 1–21, https://doi.org/10.2136/vzj2016.12.0125, 2017.

Cai, G., Vanderborght, J., Langensiepen, M., Schnepf, A., Hüging, H., and Vereecken, H.: Root growth, water uptake, and sap flow of winter wheat in response to different soil water conditions, Hydrol. Earth Syst. Sci., 22, 2449–2470, https://doi.org/10.5194/hess-22-2449-2018, 2018.

Cai, G., Ahmed, M. A., Abdalla, M., and Carminati, A.: Root hydraulic phenotypes impacting water uptake in drying soils, Plant Cell Environ., 45, 650–663, https://doi.org/10.1111/pce.14259, 2022a.

Cai, G., König, M., Carminati, A., Abdalla, M., Javaux, M., Wankmüller, F., and Ahmed, M. A.: Transpiration response to soil drying and vapor pressure deficit is soil texture specific, Plant Soil, 500, 129–145, https://doi.org/10.1007/s11104-022-05818-2, 2022b.

Cai, Q., Zhang, Y., Sun, Z., Zheng, J., Bai, W., Zhang, Y., Liu, Y., Feng, L., Feng, C., Zhang, Z., Yang, N., Evers, J. B., and Zhang, L.: Morphological plasticity of root growth under mild water stress increases water use efficiency without reducing yield in maize, Biogeosciences, 14, 3851–3858, https://doi.org/10.5194/bg-14-3851-2017, 2017.

Carminati, A. and Javaux, M.: Soil Rather Than Xylem Vulnerability Controls Stomatal Response to Drought, Trends Plant Sci., 25, 868–880, https://doi.org/10.1016/j.tplants.2020.04.003, 2020.

Carminati, A., Zarebanadkouki, M., Kroener, E., Ahmed, M. A., and Holz, M.: Biophysical rhizosphere processes affecting root water uptake, Ann. Bot., 118, 561–571, https://doi.org/10.1093/aob/mcw113, 2016.

Choudhary, S. and Sinclair, T. R.: Hydraulic conductance differences among sorghum genotypes to explain variation in restricted transpiration rates, Funct. Plant Biol., 41, 270–275, https://doi.org/10.1071/FP13246, 2014.

Couvreur, V., Vanderborght, J., Draye, X., and Javaux, M.: Dynamic aspects of soil water availability for isohydric plants: Focus on root hydraulic resistances, Water Resour. Res., 50, 8891–8906, https://doi.org/10.1002/2014WR015608, 2014.

Daryanto, S., Wang, L., and Jacinthe, P.: Global Synthesis of Drought Effects on Maize and Wheat Production, PLoS One, 11, 1–15, https://doi.org/10.1371/journal.pone.0156362, 2016.

Domec, J. and Pruyn, M. L.: Bole girdling affects metabolic properties and root , trunk and branch hydraulics of young ponderosa pine trees, Tree Physiol., 28, 1493–1504, 2008.

Draye, X., Kim, Y., Lobet, G., and Javaux, M.: Model-assisted integration of physiological and environmental constraints affecting the dynamic and spatial patterns of root water uptake from soils, J. Exp. Bot., 61, 2145–2155, https://doi.org/10.1093/jxb/erq077, 2010.

Dynamax: Dynagage Sap Flow Sensor User Manual, 106, https://www.dynamax.com (last access: 3 May 2015), 2005.

Fang, J. and Su, Y.: Effects of Soils and Irrigation Volume on Maize Yield, Irrigation Water Productivity, and Nitrogen Uptake, Sci. Rep., 9, 1–11, https://doi.org/10.1038/s41598-019-41447-z, 2019.

Frensch, J. and Steudle, E.: Axial and Radial Hydraulic Resistance to Roots of Maize (Zea mays L.), Plant Physiol., 91, 719–726, 1989.

Gallardo, M., Eastham, J., Gregory, P. J., and Turner, N. C.: A comparison of plant hydraulic conductances in wheat and lupins, J. Exp. Bot., 47, 233–239, https://doi.org/10.1093/jxb/47.2.233, 1996.

Hochberg, U., Rockwell, F. E., Holbrook, N. M., and Cochard, H.: Iso/Anisohydry: A Plant–Environment Interaction Rather Than a Simple Hydraulic Trait, Trends Plant Sci., 23, 112–120, https://doi.org/10.1016/j.tplants.2017.11.002, 2018.

Hopmans, J. W. and Bristow, K. L.: Current Capabilities and Future Needs of Root Water and Nutrient Uptake Modeling, Adv. Agron., 77, 103–183, https://doi.org/10.1016/S0065-2113(02)77014-4, 2002.

Hubbard, R. M., Ryan, M. G., Stiller, V., and Sperry, J. S.: Stomatal conductance and photosynthesis vary linearly with plant hydraulic conductance in ponderosa pine, Plant Cell Environ., 24, 113–121, https://doi.org/10.1046/j.1365-3040.2001.00660.x, 2001.

IPCC: Climate Change 2022: Impacts, Adaptation, and Vulnerability, in: Contribution of Working Group II to the Sixth Assessment Report of the Intergovernmental Panel on Climate Change, edited by: Pörtner, H.-O., Roberts, D. C., Tignor, M., Poloczanska, E. S., Mintenbeck, K., Alegría, A., Craig, M., Langsdorf, S., Löschke, S., Möller, V., Okem, A., and Rama, B., Cambridge University Press, Cambridge University Press, Cambridge, UK and New York, NY, USA, 3056 pp., https://doi.org/10.1017/9781009325844, 2022.

Jorda, H., Ahmed, M. A., Javaux, M., Carminati, A., Duddek, P., Vetterlein, D., and Vanderborght, J.: Field scale plant water relation of maize (Zea mays) under drought – impact of root hairs and soil texture, Plant Soil, 478, 59–84, https://doi.org/10.1007/s11104-022-05685-x, 2022.

Koehler, T., Moser, D. S., Botezatu, Á., Murugesan, T., Kaliamoorthy, S., Zarebanadkouki, M., Bienert, M. D., Bienert, G. P., Carminati, A., Kholová, J., and Ahmed, M.: Going underground: soil hydraulic properties impacting maize responsiveness to water deficit, Plant Soil, 478, 43–58, https://doi.org/10.1007/s11104-022-05656-2, 2022.

Lärm, L., Bauer, F. M., Hermes, N., van der Kruk, J., Vereecken, H., Vanderborght, J., Nguyen, T. H., Lopez, G., Seidel, S. J., Ewert, F., Schnepf, A., and Klotzsche, A.: Multi-year belowground data of minirhizotron facilities in Selhausen, Sci. Data, 10, 1–15, https://doi.org/10.1038/s41597-023-02570-9, 2023.

Li, X., Sinclair, T. R., and Bagherzadi, L.: Hydraulic Conductivity Changes in Soybean Plant-Soil System with Decreasing Soil Volumetric Water Content, J. Crop Improv., 30, 713–723, https://doi.org/10.1080/15427528.2016.1231729, 2016.

Meunier, F., Zarebanadkouki, M., Ahmed, M. A., Carminati, A., Couvreur, V., and Javaux, M.: Hydraulic conductivity of soil-grown lupine and maize unbranched roots and maize root-shoot junctions, J. Plant Physiol., 227, 31–44, https://doi.org/10.1016/j.jplph.2017.12.019, 2018.

Morandage, S., Vanderborght, J., Zörner, M., Cai, G., Leitner, D., Vereecken, H., and Schnepf, A.: Root architecture development in stony soils, Vadose Zone J., (April), 20, e20133, https://doi.org/10.1002/vzj2.20133, 2021.

Müllers, Y., Postma, J. A., Poorter, H., and van Dusschoten, D.: Stomatal conductance tracks soil-to-leaf hydraulic conductance in faba bean and maize during soil drying, Plant Physiol., 190, 2279–2294, https://doi.org/10.1093/plphys/kiac422, 2022.

Nguyen, T. H., Langensiepen, M., Vanderborght, J., Hüging, H., Mboh, C. M., and Ewert, F.: Comparison of root water uptake models in simulating $CO_2$ and $H_2O$ fluxes and growth of wheat, Hydrol. Earth Syst. Sci., 24, 4943–4969, https://doi.org/10.5194/hess-24-4943-2020, 2020.

Nguyen, T. H., Langensiepen, M., Hueging, H., Gaiser, T., Seidel, S. J., and Ewert, F.: Expansion and evaluation of two coupled root–shoot models in simulating $CO_2$ and $H_2O$ fluxes and growth of maize, Vadose Zone J., 21, 1–31, https://doi.org/10.1002/vzj2.20181, 2022a.

Nguyen, T. H., Langensiepen, M., Gaiser, T., Webber, H., Ahrends, H., Hueging, H., and Ewert, F.: Responses

of winter wheat and maize to varying soil moisture: From leaf to canopy, Agr. Forest Meteorol., 314, 108803, https://doi.org/10.1016/j.agrformet.2021.108803, 2022b.

Nguyen, T., Lopez, G., Seidel, S., Lärm, Lena, Bauer, Felix, Klotzsche, Anja, Schnepf, A., Gaiser, T., Hüging, H., and Ewert, F.: Multi-year aboveground data of minirhizotron facilities in Selhausen, TERENO [data set], https://doi.org/10.34731/1a9s-ax66, 2024.

Ordóñez, R. A., Archontoulis, S. V., Martinez-Feria, R., Hatfield, J. L., Wright, E. E., and Castellano, M. J.: Root to shoot and carbon to nitrogen ratios of maize and soybean crops in the US Midwest, Eur. J. Agron., 120, 126130, https://doi.org/10.1016/j.eja.2020.126130, 2020.

Ranawana, S. R. W. M. C. J. K., Siddique, K. H. M., Palta, J. A., Stefanova, K., and Bramley, H.: Stomata coordinate with plant hydraulics to regulate transpiration response to vapour pressure deficit in wheat, Funct. Plant Biol., 48, 839–850, https://doi.org/10.1071/FP20392, 2021.

R Core Team: R: A Language and Environment for Statistical Computing, R Foundation for Statistical Computing, Vienna, https://www.R-project.org (last access: 8 December 2024), 2022.

Richards, R. A., Rebetzke, G. J., Condon, A. G., and van Herwaarden, A. F.: Breeding Opportunities for Increasing the Efficiency of Water Use and Crop Yield in Temperate Cereals, Crop Sci., 42, 111–121, https://doi.org/10.2135/cropsci2002.1110, 2002.

Rodriguez-Dominguez, C. M. and Brodribb, T. J.: Declining root water transport drives stomatal closure in olive under moderate water stress, New Phytol., 225, 126–134, https://doi.org/10.1111/nph.16177, 2020.

Scharwies, J. D. and Dinneny, J. R.: Water transport, perception, and response in plants, J. Plant Res., 132, 311–324, https://doi.org/10.1007/s10265-019-01089-8, 2019.

Sinclair, T. R. and Ludlow, M. M.: Influence of soil water supply on the plant water balance of four tropical grain legumes, Aust. J. Plant Physiol., 13, 329–341, 1986.

Stadler, A., Rudolph, S., Kupisch, M., Langensiepen, M., van der Kruk, J., and Ewert, F.: Quantifying the effects of soil variability on crop growth using apparent soil electrical conductivity measurements, Eur. J. Agron., 64, 8–20, https://doi.org/10.1016/j.eja.2014.12.004, 2015.

Sulis, M., Couvreur, V., Keune, J., Cai, G., Trebs, I., Junk, J., Shrestha, P., Simmer, C., Kollet, S. J., Vereecken, H., and Vanderborght, J.: Incorporating a root water uptake model based on the hydraulic architecture approach in terrestrial systems simulations, Agr. Forest Meteorol., 269–270, 28–45, https://doi.org/10.1016/j.agrformet.2019.01.034, 2019.

Sunita, C., Sinclair, T. R., Messina, C. D., and Cooper, M.: Hydraulic conductance of maize hybrids differing in transpiration response to vapor pressure deficit, Crop Sci., 54, 1147–1152, https://doi.org/10.2135/cropsci2013.05.0303, 2014.

Tardieu, F.: Too many partners in root – shoot signals. Does hydraulics qualify as the only signal that feeds back over time for reliable stomatal, New Phytol., 212, 802–804, 2016.

Tardieu, F. and Simonneau, T.: Variability among species of stomatal control under fluctuating soil water status and evaporative demand: modelling isohydric and anisohydric behaviours, J. Exp. Bot., 49, 419–432, https://doi.org/10.1093/jxb/49.Special_Issue.419, 1998.

Tardieu, F., Draye, X., and Javaux, M.: Root Water Uptake and Ideotypes of the Root System: Whole-Plant Controls Matter, Vadose Zone J., 16, 1–10, https://doi.org/10.2136/vzj2017.05.0107, 2017.

TERENO: Data Discovery Portal, TERENO, https://www.tereno.net/ddp/dispatch?searchparams=freetext-Selhausen, last access: October 2020.

Trillo, N. and Fernández, R. J.: Wheat plant hydraulic properties under prolonged experimental drought: Stronger decline in root-system conductance than in leaf area, Plant Soil, 277, 277–284, https://doi.org/10.1007/s11104-005-7493-5, 2005.

Tsuda, M. and Tyree, M. T.: Whole-plant hydraulic resistance and vulnerability segmentation in Acer saccharinum, Tree Physiol., 17, 351–357, 1997.

Vadez, V.: Root hydraulics: The forgotten side of roots in drought adaptation, F. Crop. Res., 165, 15–24, 2014.

Vadez, V., Choudhary, S., Kholová, J., Hash, C. T., Srivastava, R., Kumar, A. A., Prandavada, A., and Anjaiah, M.: Transpiration efficiency: Insights from comparisons of C4cereal species, J. Exp. Bot., 72, 5221–5234, https://doi.org/10.1093/jxb/erab251, 2021.

Vanderborght, J., Graf, A., Steenpass, C., Scharnagl, B., Prolingheuer, N., Herbst, M., Franssen, H. H., and Vereecken, H.: Within-Field Variability of Bare Soil Evapora O on Derived from Eddy Covariance Measurements, Vadose Zone J., 9, 943–954, https://doi.org/10.2136/vzj2009.0159, 2010.

Vereecken, H., Schnepf, A., Hopmans, J. W., Javaux, M., Or, D., Roose, T., Vanderborght, J., Young, M. H., Amelung, W., Aitkenhead, M., Allison, S. D., Assouline, S., Baveye, P., Berli, M., Brüggemann, N., Finke, P., Flury, M., Gaiser, T., Govers, G., Ghezzehei, T., Hallett, P., Hendricks Franssen, H. J., Heppell, J., Horn, R., Huisman, J. A., Jacques, D., Jonard, F., Kollet, S., Lafolie, F., Lamorski, K., Leitner, D., McBratney, A., Minasny, B., Montzka, C., Nowak, W., Pachepsky, Y., Padarian, J., Romano, N., Roth, K., Rothfuss, Y., Rowe, E. C., Schwen, A., Šimůnek, J., Tiktak, A., Van Dam, J., van der Zee, S. E. A. T. M., Vogel, H. J., Vrugt, J. A., Wöhling, T., and Young, I. M.: Modeling Soil Processes: Review, Key Challenges, and New Perspectives, Vadose Zone J., 15, vzj2015.09.0131, https://doi.org/10.2136/vzj2015.09.0131, 2016.

Vetterlein, D., Phalempin, M., Lippold, E., Schlüter, S., Schreiter, S., Ahmed, M. A., Carminati, A., Duddek, P., Jorda, H., Bienert, G. P., Bienert, M. D., Tarkka, M., Ganther, M., Oburger, E., Santangeli, M., Javaux, M., and Vanderborght, J.: Root hairs matter at field scale for maize shoot growth and nutrient uptake, but root trait plasticity is primarily triggered by texture and drought, Plant Soil, 478, 119–141, https://doi.org/10.1007/s11104-022-05434-0, 2022.

Vitale, L., Di Tommasi, P., Arena, C., Fierro, A., Virzo De Santo, A., and Magliulo, V.: Effects of water stress on gas exchange of field grown Zea mays L. in Southern Italy: An analysis at canopy and leaf level, Acta Physiol. Plant., 29, 317–326, https://doi.org/10.1007/s11738-007-0041-6, 2007.

Wang, N., Gao, J., and Zhang, S.: Overcompensation or limitation to photosynthesis and root hydraulic conductance altered by rehydration in seedlings of sorghum and maize, Crop J., 5, 337–344, https://doi.org/10.1016/j.cj.2017.01.005, 2017.

Welcker, C., Sadok, W., Dignat, G., Renault, M., Salvi, S., Charcosset, A., and Tardieu, F.: A common genetic determinism for sensitivities to soil water deficit and evapora-

tive demand: Meta-analysis of quantitative trait loci and introgression lines of maize, Plant Physiol., 157, 718–729, https://doi.org/10.1104/pp.111.176479, 2011.

Zhuang, J., Jin, Y., and Miyazaki, T.: Estimating water retention characteristic from soil particle-size distribution using a non-similar media concept, Soil Sci., 166, 308–321, 2001.

Zwieniecki, M. A., Melcher, P. J., Boyce, C. K., Sack, L., and Holbrook, N. M.: Hydraulic architecture of leaf venation in Laurus nobilis L., Plant, Cell Environ., 25, 1445–1450, https://doi.org/10.1046/j.1365-3040.2002.00922.x, 2002.